Report No. RF-TR-63-23

COPY 19

THE EFFECTS OF BASE BLEED AND SUSTAINER ROCKET NOZZLE DIAMETER AND LOCATION ON THE BASE DRAG OF A BODY OF REVOLUTION WITH CONCENTRIC BOOST AND SUSTAINER ROCKET NOZZLES

15 July 1963

U S ARMY MISSILE COMMAND
REDSTONE ARSENAL, ALABAMA

RSA FORM 1385, 1 JAN 63 PREVIOUS EDITION IS OBSOLETE

DDC Availability Notice

Qualified requesters may obtain copies of this report from the Defense Documentation Center for Scientific and Technical Information, Cameron Station, Alexandria, Virginia, 22314.

Destruction Notice

Destroy; do not return.

15 July 1963

Report No. RF-TR-63-23

THE EFFECTS OF BASE BLEED AND SUSTAINER ROCKET NOZZLE DIAMETER AND LOCATION ON THE BASE DRAG OF A BODY OF REVOLUTION WITH CONCENTRIC BOOST AND SUSTAINER ROCKET NOZZLES

By

Charles E. Brazzel

AMC Management Structure Code No. 5210.11.148

Aerodynamics Branch
Advanced Systems Laboratory
Future Missile Systems Division
Directorate of Research and Development
U.S. Army Missile Command
Redstone Arsenal, Alabama

ABSTRACT

A concentric arrangement of boost and sustainer rocket nozzles has been investigated to determine the effects of base bleed and the effects of sustainer nozzle diameter and relative longitudinal position on the base drag of the body during sustainer operation. The results of the investigation indicate that the jet-on base drag of a body can be significantly reduced by the use of base bleed and nozzle arrangement, and that the jet-on base drag is a function of the jet thrust.

The data presented are based on the results of tests in the Aberdeen Ballistic Research Laboratories 13 by 15 inch supersonic wind tunnel at Mach numbers of 2.0 and 2.5. The model tested had sustainer nozzle-to-base diameter ratios of 0.10, 0.20, and 0.30, and boost nozzle-to-base diameter ratio of 0.80. The sustainer nozzle was tested at longitudinal positions between 0.60 calibers aft to 0.98 calibers forward of the base.

TABLE OF CONTENTS

LIST OF ILLUSTRATIONS

LIST OF SYMBOLS

C_{D_B}	Base drag coefficient based on integration of pressure distributions over the total base area excluding the sustainer nozzle exit area and referenced to the total base area
C_T	Thrust coefficient = Thrust/q_{∞} x Reference Area
d_n	Sustainer nozzle exit diameter
D_B	Body base diameter
M	Mach number
$\dot{m}_b$	Bleed mass flow
$\dot{m}_j$	Sustainer nozzle mass flow
$\dot{m}_{\infty}$	Body stream-tube mass flow
p	Local static pressure
p_b	Average base pressure, integrated over total base area excluding sustainer nozzle exit area
p_c	Sustainer nozzle chamber pressure
p_j	Sustainer nozzle exit static pressure
p_{∞}	Free-stream static pressure
q_{∞}	Free-stream dynamic pressure
V	Velocity
X	Distance from base of model
X_n	Distance from base of model to base of sustainer nozzle (Forward is positive.)

I. INTRODUCTION

Several potential applications exist in land combat and air defense weapons systems for boost-sustain propulsion. One of the advantages for this type of propulsion lies in the increase in missile performance arising from energy management considerations. As a part of the overall problem, it is necessary to investigate techniques for minimizing missile base drag. Current methods allow prediction and optimization of body forebody and friction drag with a reasonable degree of accuracy; however, methods are not available for reliably predicting the base drag of a body with an operating jet. The jet-on base drag of a body can be as high as 50 percent of the total drag; therefore techniques for predicting the jet-on base drag are needed for proper design and evaluation of the aerodynamic-propulsion configuration of missiles during sustainer operation.

This report presents the results of the second phase of a study on base drag reduction conducted as a part of SR Project, Base Drag Reduction, Code 5210.11.148. A body with concentric boost and sustainer rocket nozzles has been studied to determine the effects of base bleed, and the effects of sustainer nozzle diameter and position on the body base drag. The results of the first phase of the study have been presented in Reference 1.

The data presented in this report are based on the results of wind tunnel tests at Mach numbers 2.0 and 2.5. Parameters varied during the tests were Mach number, base bleed, nozzle diameter, nozzle position, and sustainer nozzle chamber pressure. The boost nozzle was inactive and the sustainer jet was simulated with air. The configuration tested was a body of revolution with an ogive nose and a cylindrical afterbody.

II. APPARATUS AND PROCEDURE

The test was conducted in Tunnel No. 1 of the Ballistic Research Laboratories, Aberdeen Proving Grounds, Maryland. That facility is a continuous flow, supersonic wind tunnel capable of operating at Mach numbers from 1.2 to 5.0, and has a test section 13 inches wide by 15 inches high.

The model tested was a body of revolution with a 4-caliber, tangent ogive nose, and a 2-caliber cylindrical afterbody. It was mounted from the tunnel ceiling at 0° angle of attack by a rigid strut containing the instrumentation and air supply lines. A sustainer rocket nozzle, concentric to a boost rocket nozzle, could be tested at any of ten longitudinal

positions between, -.60 and +.98 calibers from the base of the body. The sustainer nozzles had exit diameters of 0.10, 0.20, and 0.30 calibers and were designed for an exit Mach number of 2.7 ($p_j/p_c = 0.0427$). The sustainer jet was simulated with dry air, and the boost nozzle was inactive. During the bleed runs, air was bled from the sustainer chamber to the boost nozzle chamber through orifices in the sustainer nozzle chamber wall. The amount of bleed air was varied by varying the size and number of bleed orifices. Figure 1 presents sketches of the model installation and geometry.

The base of the model was instrumented with pressure orifices along the body just forward of the base, on the base annulus, and along the interior of the boost nozzle as shown in Figure 1. Pressures at the orifices were measured with pressure transducers. Sustainer air supply pressure (p_c) was measured at an orifice in the settling chamber upstream of the nozzle throat.

During each run the sustainer supply pressure was varied while holding constant the test section Mach number, test section static pressure, sustainer nozzle position, and ratio of bleed to sustainer jet mass flow. Data recorded were test section stagnation pressure and temperature, sustainer air supply pressure, model orifice pressures, and transducer reference pressure. Accuracies of the data obtained are the following:

Mach number	±.002
Local model pressures	±.0125 psi
Sustainer supply pressure	
0 - 15 psi range	±.030 psi
0 - 100 psi range	±.200 psi
0 - 320 psi range	±.600 psi

The model local pressures were reduced to pressure coefficient and pressure ratio form, and the base drag coefficients were computed by integrating the base pressure distributions where:

$$C_{D_B} = \frac{1}{S_B} \sum a_i C_{p_i}$$

and S_B = Total base area

a_i = Incremental area

C_{p_i} = Local pressure coefficient

A more detailed discussion of the test apparatus and test procedure as well as the basic data from the test is presented in Reference 2.

III. RESULTS

The wind tunnel test results from Reference 2 have been analyzed to determine the effects of the various test parameters on base drag. The analysis is limited to values of sustainer chamber pressures sufficient to completely fill the sustainer nozzle. Although the test configuration has an inactive boost rocket nozzle concentric to an active sustainer rocket nozzle, or in effect an open base, the data are comparable to data for closed base configurations except for conditions where the sustainer jet impinged on the boost nozzle wall. Subsequent references to the nozzle and jet will refer to the sustainer nozzle and jet.

Figures 2 through 5 present the basic test results and show the effects of sustainer nozzle diameter and position and the effects of base bleed on base drag as a function of jet chamber to free-stream static pressure ratio. These data exhibit a characteristic variation of base drag with jet pressure ratio which is discussed in detail and related to base wake flow in Reference 3.

A. Effect of Diameter Ratio and Mach Number

Analysis of the data for the configuration with the nozzle at the model base ($X_n/D_B = 0.0$) shows a dependence of base pressure on thrust level and jet momentum ratio which are related. Figure 6 presents base pressure ratio as a function of thrust coefficient and Figure 7 presents base pressure ratio as a function of jet momentum ratio for nozzle diameter ratios of 0.10, 0.20, and 0.30 at Mach numbers of 2.0 and 2.5. These data indicate that base pressure ratio is independent of nozzle diameter, jet pressure ratio, and free-stream conditions except for their relative inputs to the thrust coefficient or momentum ratio. Reference 1 presents data from the first series of tests of the model at Mach numbers of 2.0, 2.5, 3.0, and 3.5 for a nozzle diameter ratio of 0.24. Due to instrumentation difficulties, the accuracy of the data from Reference 1 does not approach the accuracy of the present data; however, the data are useful to indicate trends and are presented in Figure 8 as a function of thrust coefficient to illustrate the independence of jet-on base pressure on free-stream Mach number except for its input to thrust coefficient. The relationship between jet-on base pressure and thrust coefficient and momentum ratio correlates well with experimental data from sources for bodies with supersonic jets.

B. Effect of Base Bleed

Air was bled into the boost nozzle combustion chamber through orifices in the sustainer nozzle combustion chamber wall. In most cases, the bleed mass flow was sufficient to choke the boost nozzle throat. Figure 9 presents boost nozzle pressure distributions for various bleed ratios with the 0.20 diameter ratio sustainer nozzle. These data illustrate that the boost nozzle was choked for all bleed ratios except the .015 with the 0.20 diameter ratio nozzle, and provide data for convenient determination of the actual ratio of bleed mass flow to sustainer mass flow for conditions where the boost nozzle was choked. Figure 10 presents calculated values of bleed mass flow ratios based on the pressure distributions of Figure 9. For values of bleed mass flow not sufficient to choke the boost nozzle throat, nominal values are given based on orifice area ratios.

Bleeding gases into the base area increases the base pressure as a function of the bleed mass. The incremental increase in base pressure ratio due to base bleed is presented in Figure 11 as a function of the ratio of bleed mass flow to body stream-tube mass flow. The apparent Mach number effect can be removed by dividing the mass flow ratio by the free-stream velocity. Since the bleed velocity is believed to be constant, the dependence of the effect of base bleed on base pressure ratio on bleed momentum ratio is indicated. The bleed velocity at the base could not be determined from the available data, therefore the bleed momentum ratio could not be calculated. However, since the base pressure ratio without base bleed is a function of jet momentum ratio, it is not illogical to believe that the effects of base bleed are also a function of bleed momentum ratio. The boost nozzle produces some thrust due to bleed, however the effects on base pressure are far greater than the effects of bleed thrust alone.

C. Effect of Longitudinal Position

Extension of the sustainer nozzle aft of the base of the body induces an incremental increase in base pressure which varies almost linearly with nozzle position but which does not vary with nozzle diameter of jet pressure ratio. An effect of free-stream Mach number is also indicated; however, sufficient data are not available to determine the Mach number effects. Figure 12 presents the incremental increase in base pressure ratio as a function of aft nozzle position. It is anticipated that the base pressure would continue to increase with aft nozzle position until the sustainer nozzle approached the position of the jet-off trailing shock ($X_n/D_B \approx -1.20$). Since the aft nozzle positions induce an increase in base pressure which is independent of nozzle diameter

and jet pressure ratio, the base pressure cannot be correlated on a momentum ratio or a thrust coefficient basis.

Movement of the sustainer nozzle forward into the base cavity induces a corresponding decrease in base pressure until a position is reached where the sustainer jet inpinges on the boost nozzle. With jet impingement, the static pressure on the boost nozzle aft of impingement is increased due to a pressure rise across an oblique shock produced by impingement. Further movement of the sustainer into the base cavity increases the area of the boost nozzle affected and also increases the angle of impingement which in turn causes an increase in pressure rise across the oblique shock. Therefore movement of the sustainer nozzle forward after the jet has impinged causes an increase in base pressure. This effect is discussed in more detail in Reference 1. It is interesting to note that after the jet has impinged on the boost nozzle base pressure again becomes a function of momentum ratio and thrust coefficient.

Figure 13 illustrates the incremental change in base pressure ratio with nozzle position for the 0.20 d_n/D_B nozzle at $M = 2.5$ for several jet pressure ratios.

Reference 1 illustrated that, for a given nozzle position, the point of jet impingement was independent of jet pressure ratio and external conditions. Figure 14 also illustrates that the point of jet impingement is independent of nozzle diameter.

IV. CONCLUSIONS

The following conclusions can be made, based on analysis of the test data:

1. The base pressure ratio, for bodies with jets coplaner to the base, can be expressed as a function of either jet momentum ratio or thrust coefficient and is independent of nozzle diameter, jet pressure ratio, and free-stream conditions except for their respective inputs to the momentum ratio and thrust coefficient.

2. The increase in base pressure due to gases bled into the base area can be expressed as a function of the bleed mass momentum ratio and is independent of bleed area or free-stream conditions except for their respective inputs to the momentum ratio.

3. Extending the nozzle aft of the body base causes an increase in base pressure which is a function of the amount of extension and free-stream Mach number but is independent of nozzle diameter and jet pressure ratio.

4. Moving the nozzle forward into the body can increase the base pressure due to impingement of the jet on the body internal surfaces. The amount is a function of jet conditions and geometry but is independent of environmental conditions.

It is recommended that future phases of the base drag reduction study be conducted to determine the effects on jet-on base drag of the following:

1. Effects of base bleed over wide Mach number range.

2. Effects of aft nozzle extensions over wide Mach number range and for further aft extensions.

3. Effects of jet Mach number and expansion angle.

4. Effects of jet temperature and physical composition.

5. Effects of afterbody geometry.

6. Potential heating problems associated with flow impingement on the boost nozzle.

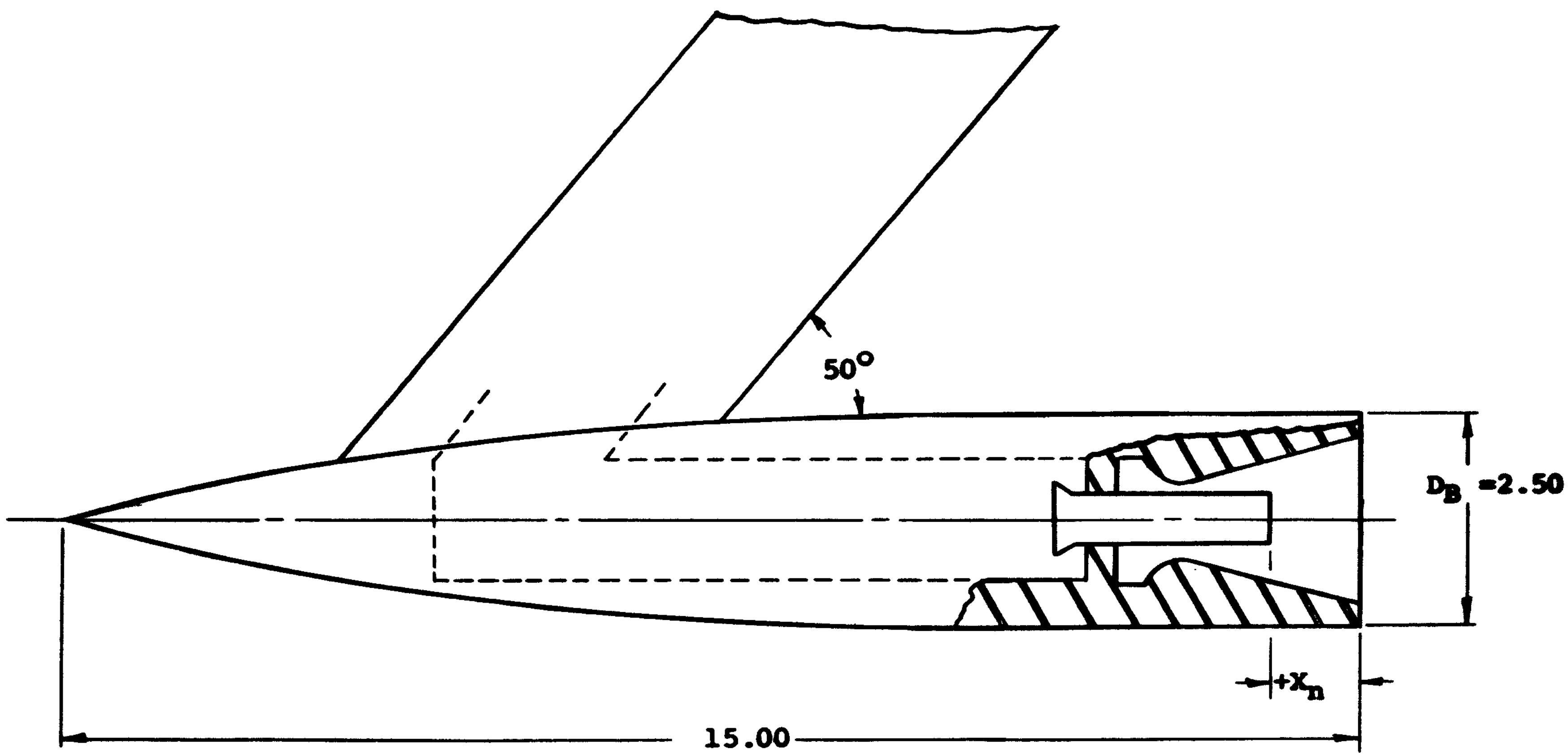

a. Model Installation

Figure 1. Model Details

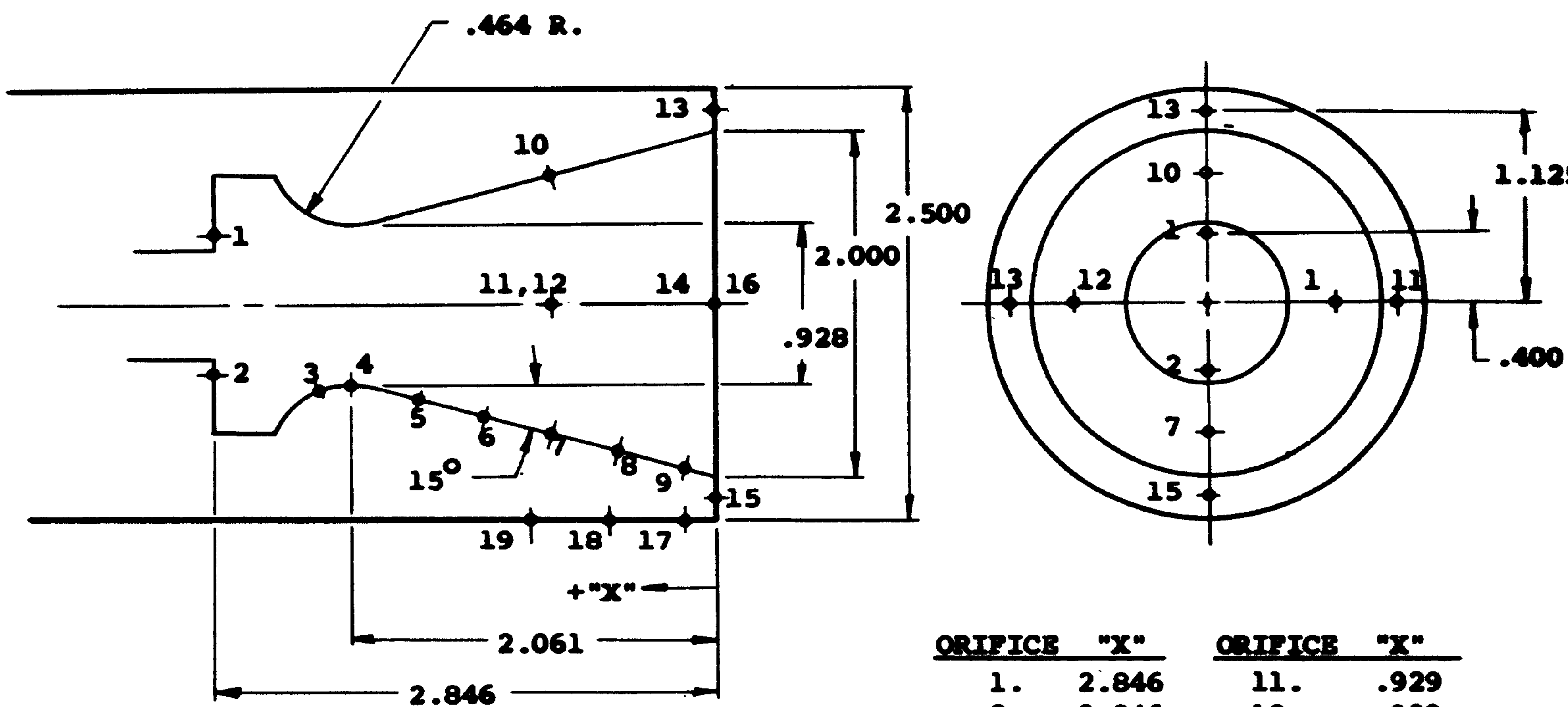

ORIFICE	"X"	ORIFICE	"X"
1.	2.846	11.	.929
2.	2.846	12.	.929
3.	2.398	13.	.000
4.	2.061	14.	.000
5.	1.685	15.	.000
6.	1.307	16.	.000
7.	.929	17.	.180
8.	.552	18.	1.060
9.	.174	19.	2.060
10.	.929		

b. Boost Nozzle Geometry

Figure 1. Continued

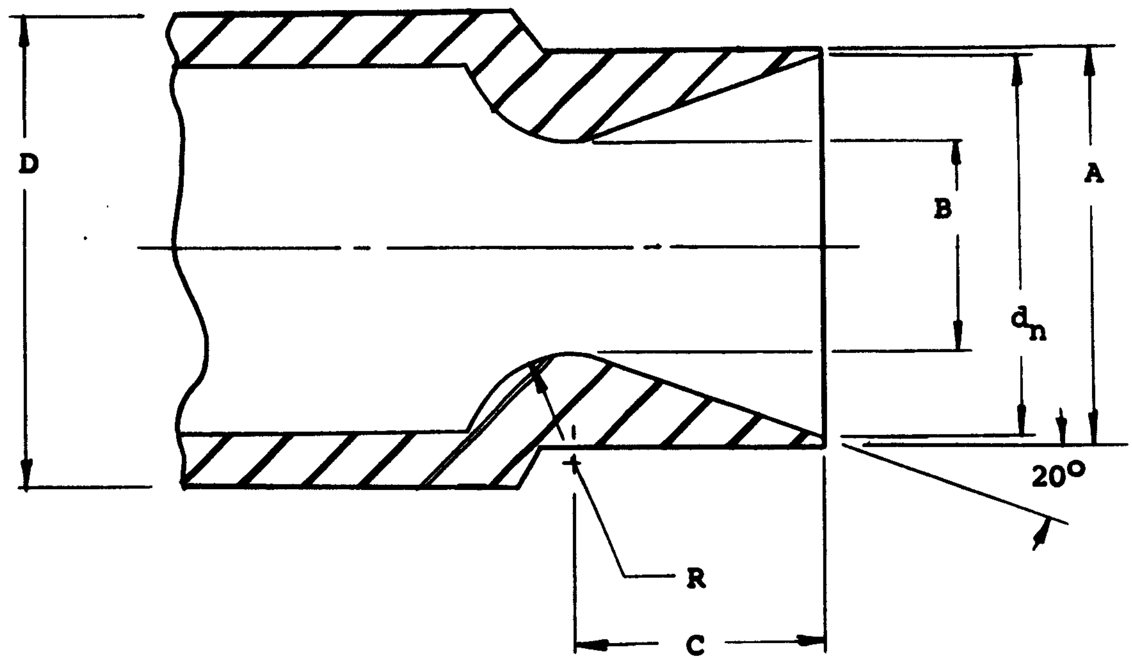

d_n/D_B	d_n	A	B	C	D	R
0.10	0.250	0.27	0.140	0.163	0.623	0.070
0.20	0.500	0.52	0.280	0.327	0.623	0.140
0.30	0.750	0.79	0.420	0.490	0.623	0.210

c. Sustainer Nozzle Geometry

Figure 1. Concluded

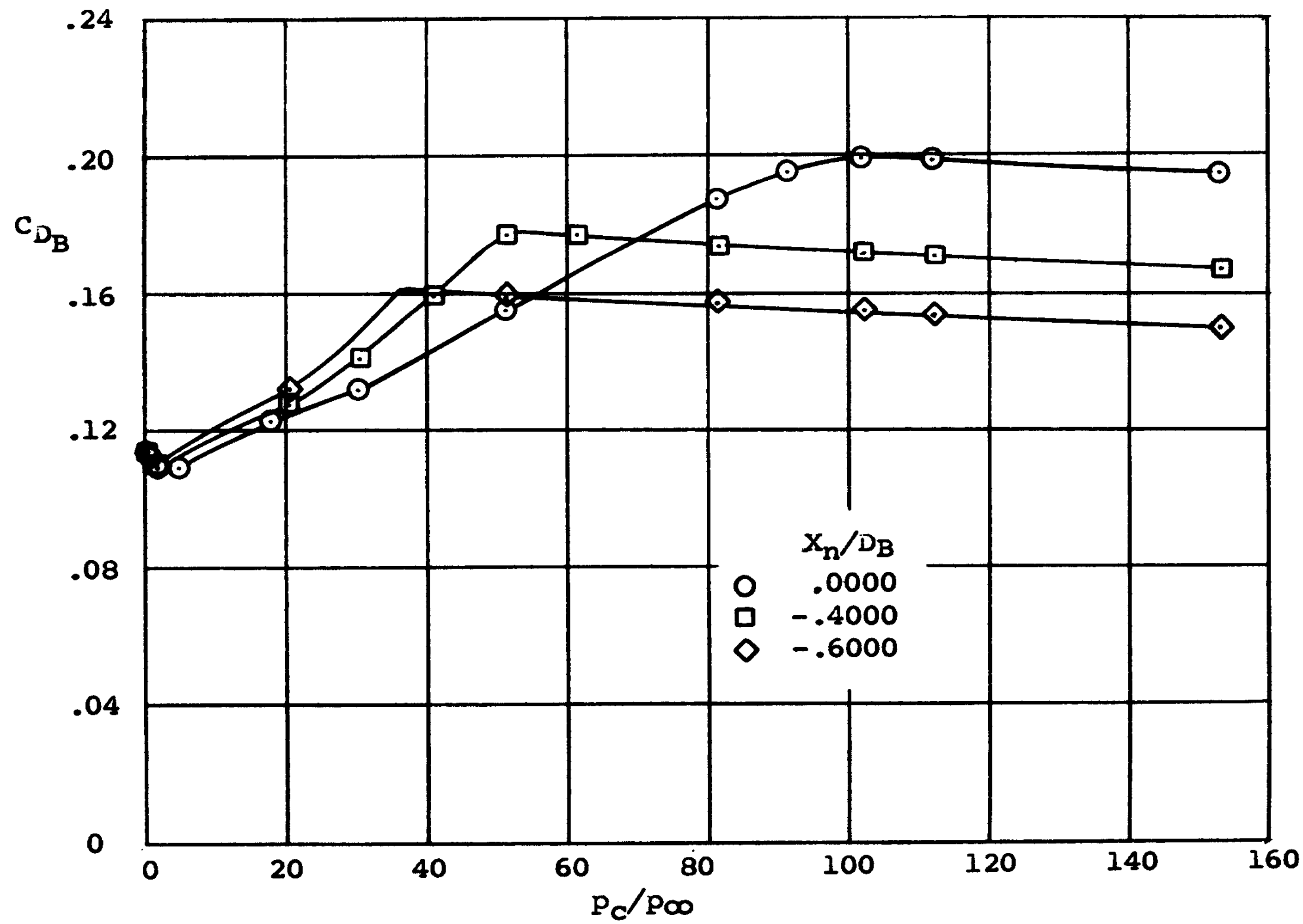

a. Aft Nozzle Positions

Figure 2. Effects of Sustainer Nozzle Position on Base Drag. $d_n/D_B = 0.10$; $M = 2.5$

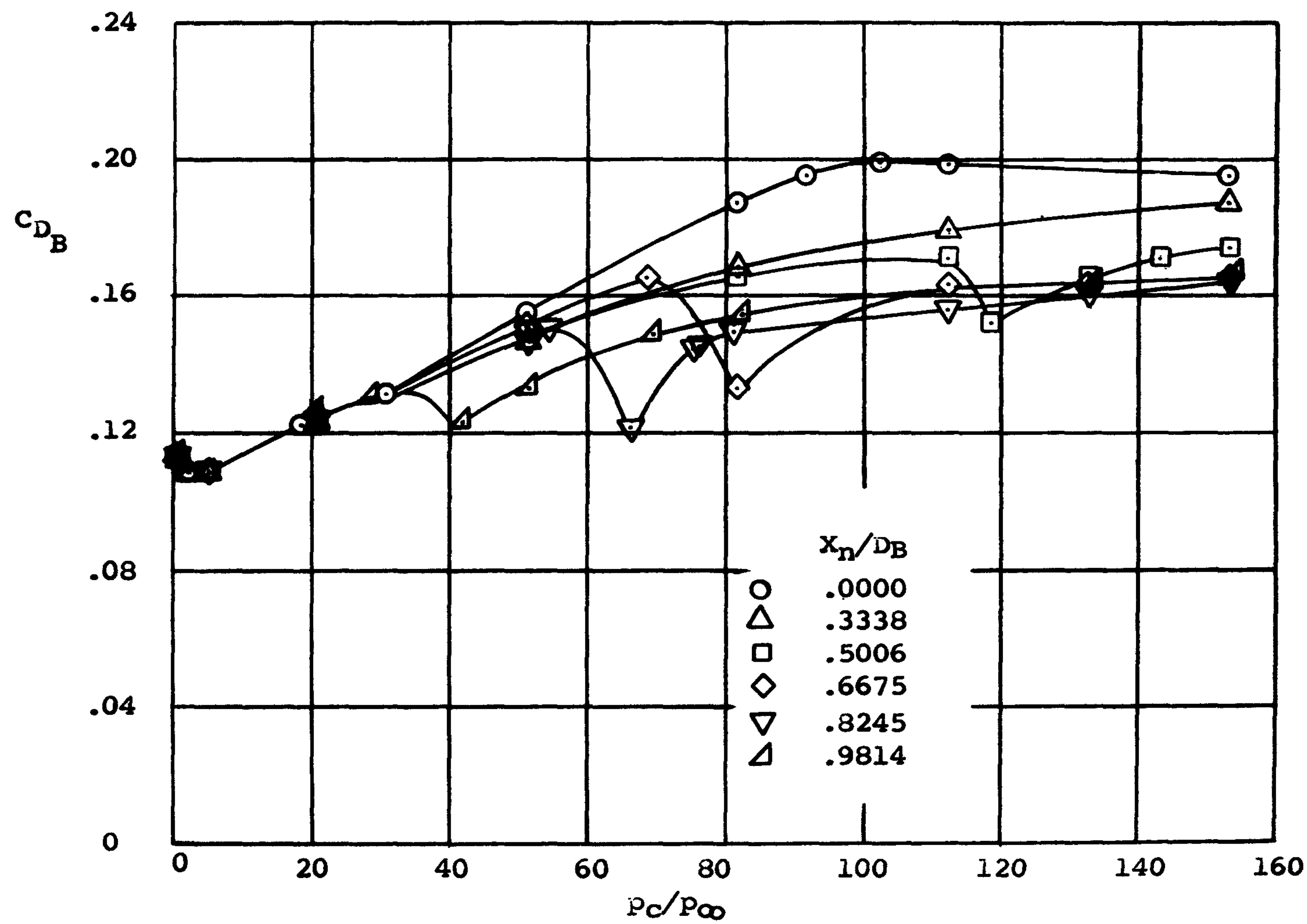

b. Forward Nozzle Positions

Figure 2. Continued

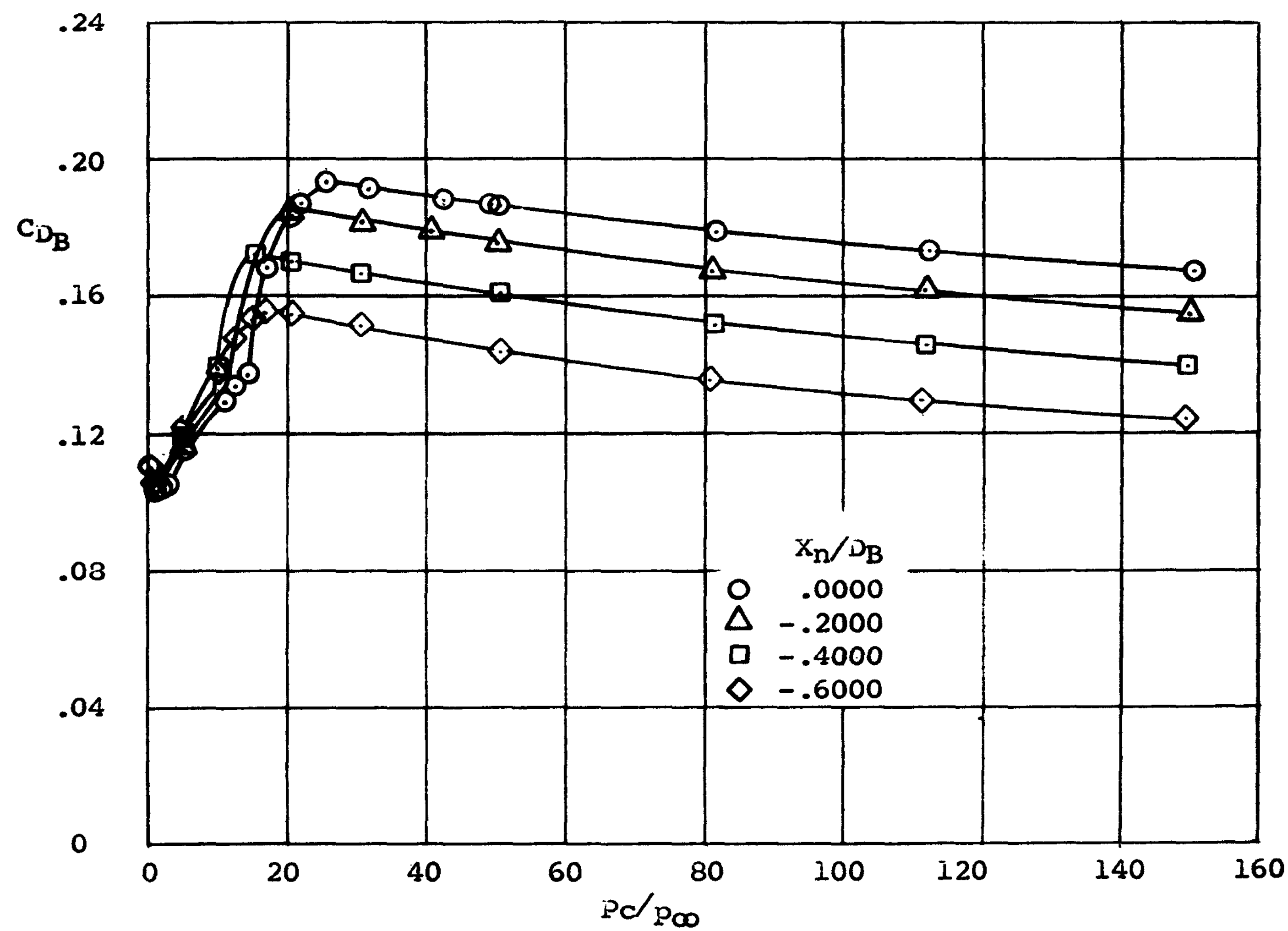

a. Aft Nozzle Positions

Figure 3. Effects of Sustainer Nozzle Position on Base Drag. $d_n/D_B = 0.20$; $M = 2.5$

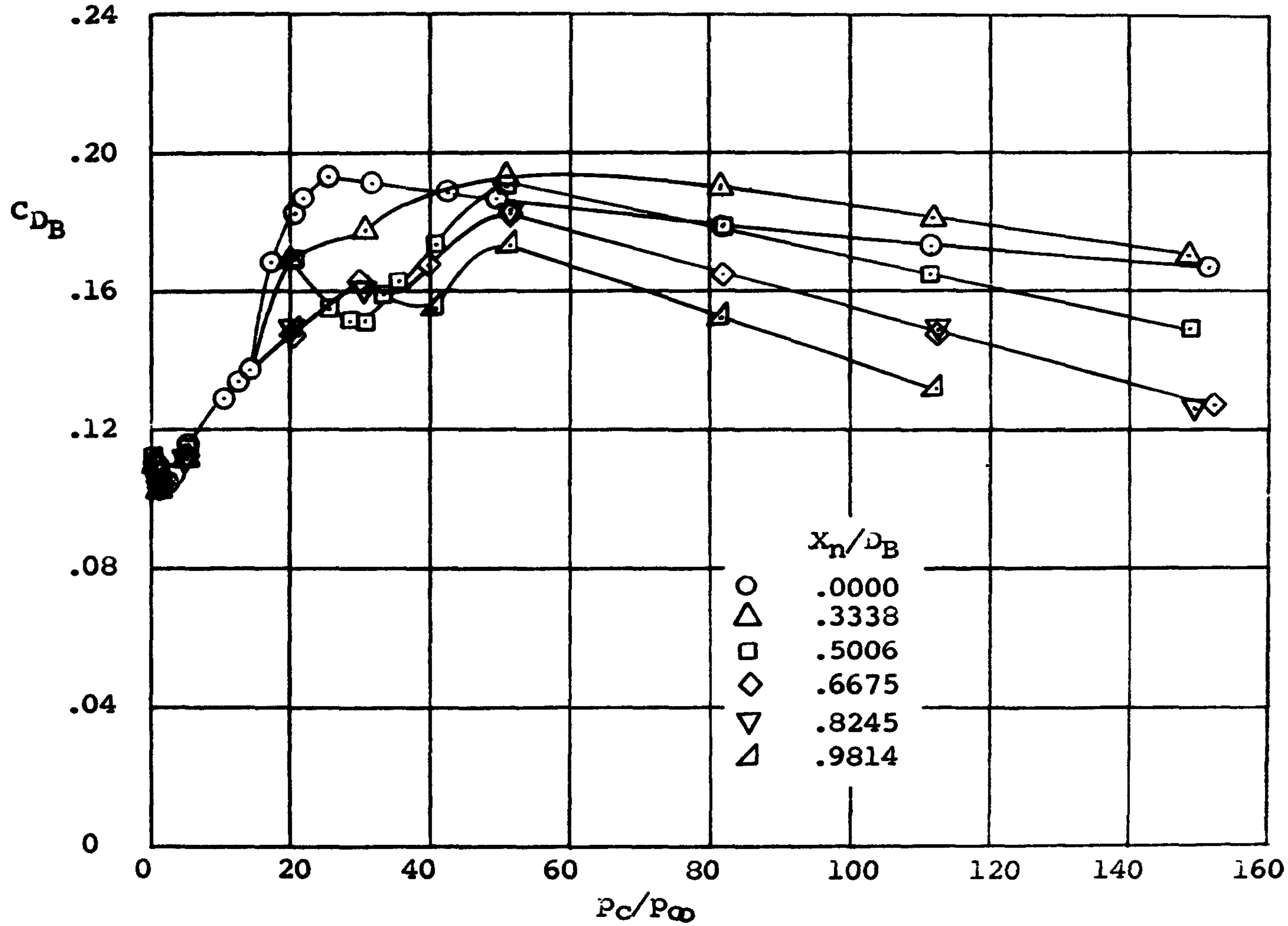

b. Forward Nozzle Positions

Figure 3. Continued

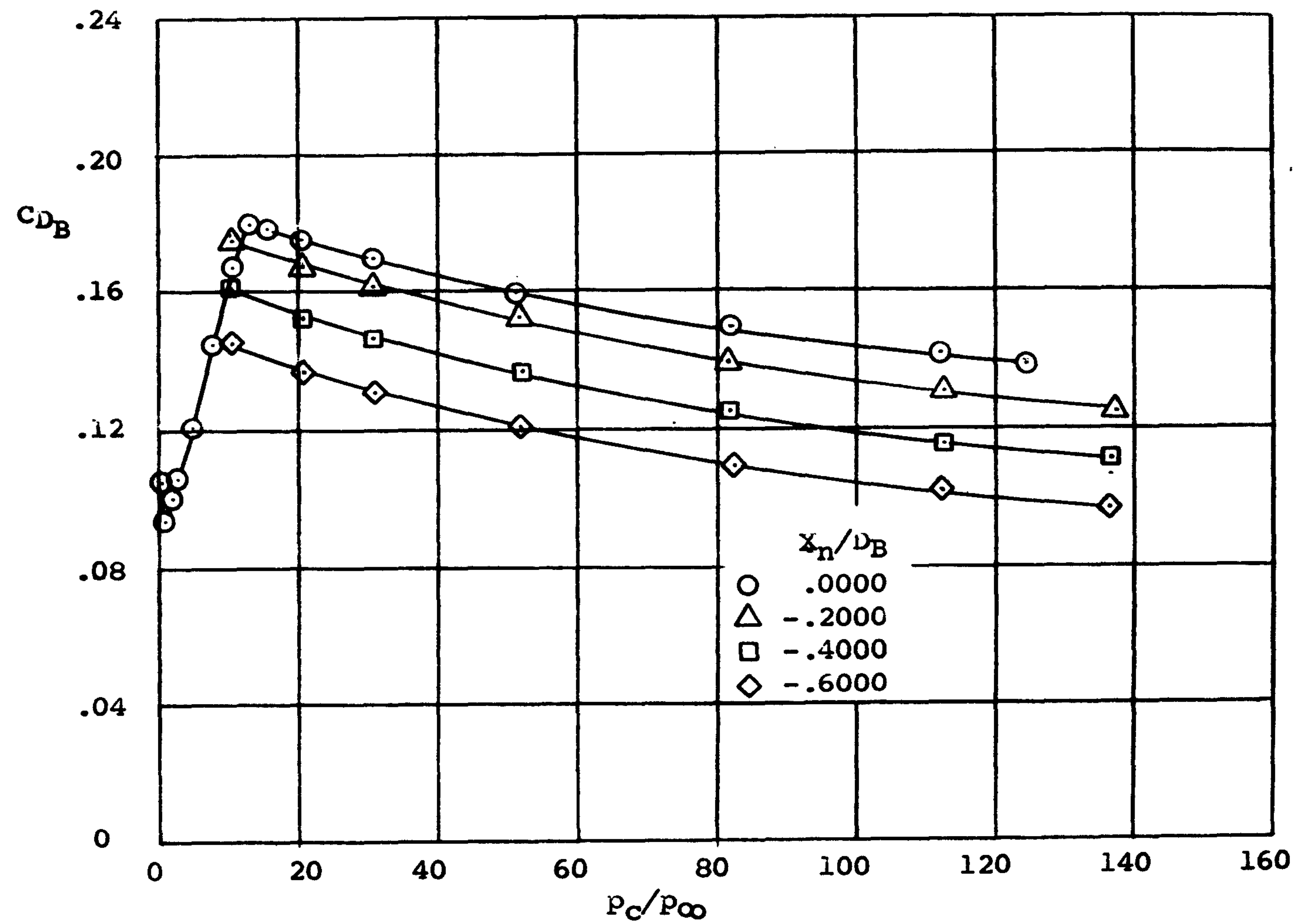

a. Aft Nozzle Positions

Figure 4. Effects of Sustainer Nozzle Position on Base Drag. $d_n/D_B = 0.30$; $M = 2.5$

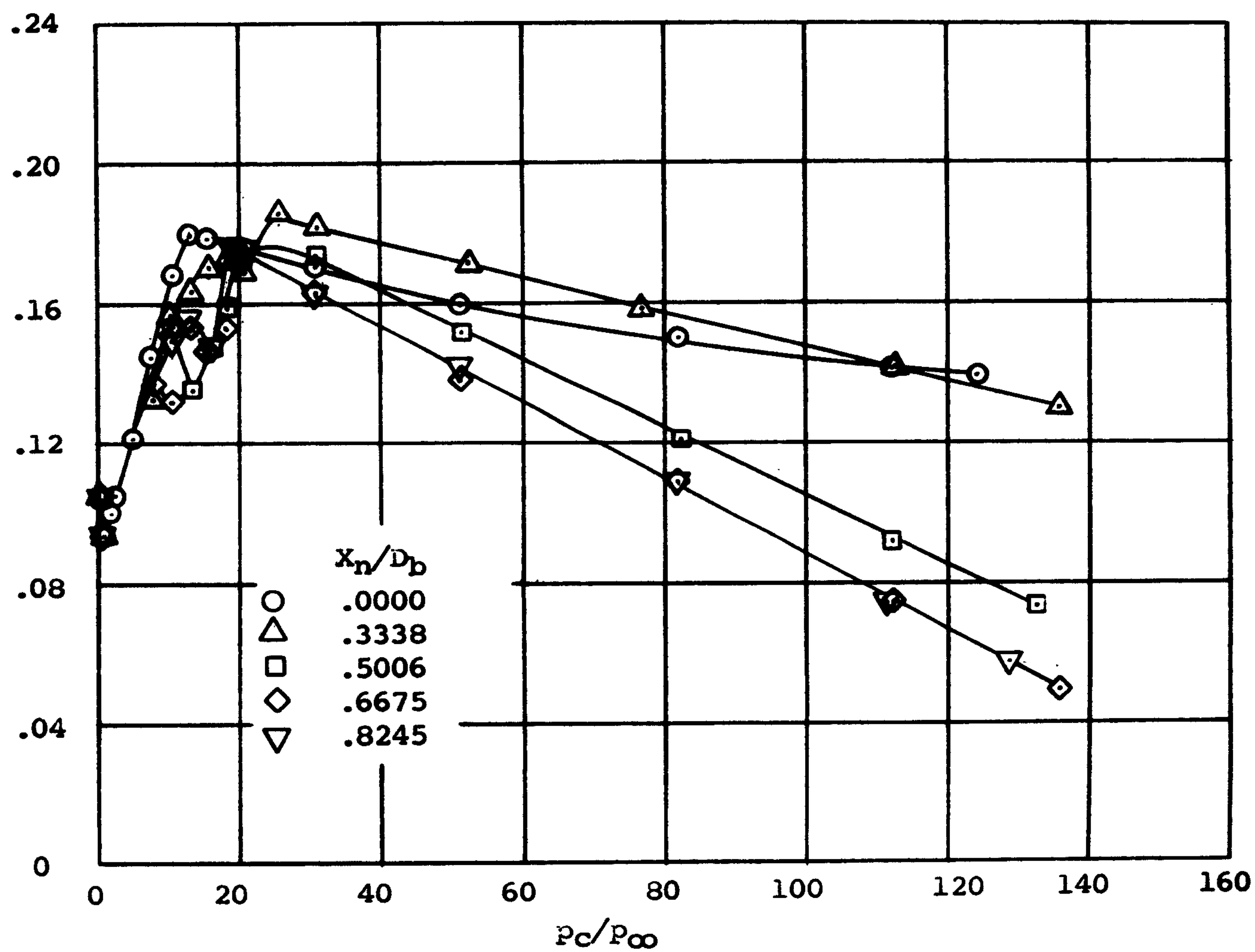

b. Forward Nozzle Positions

Figure 4. Continued

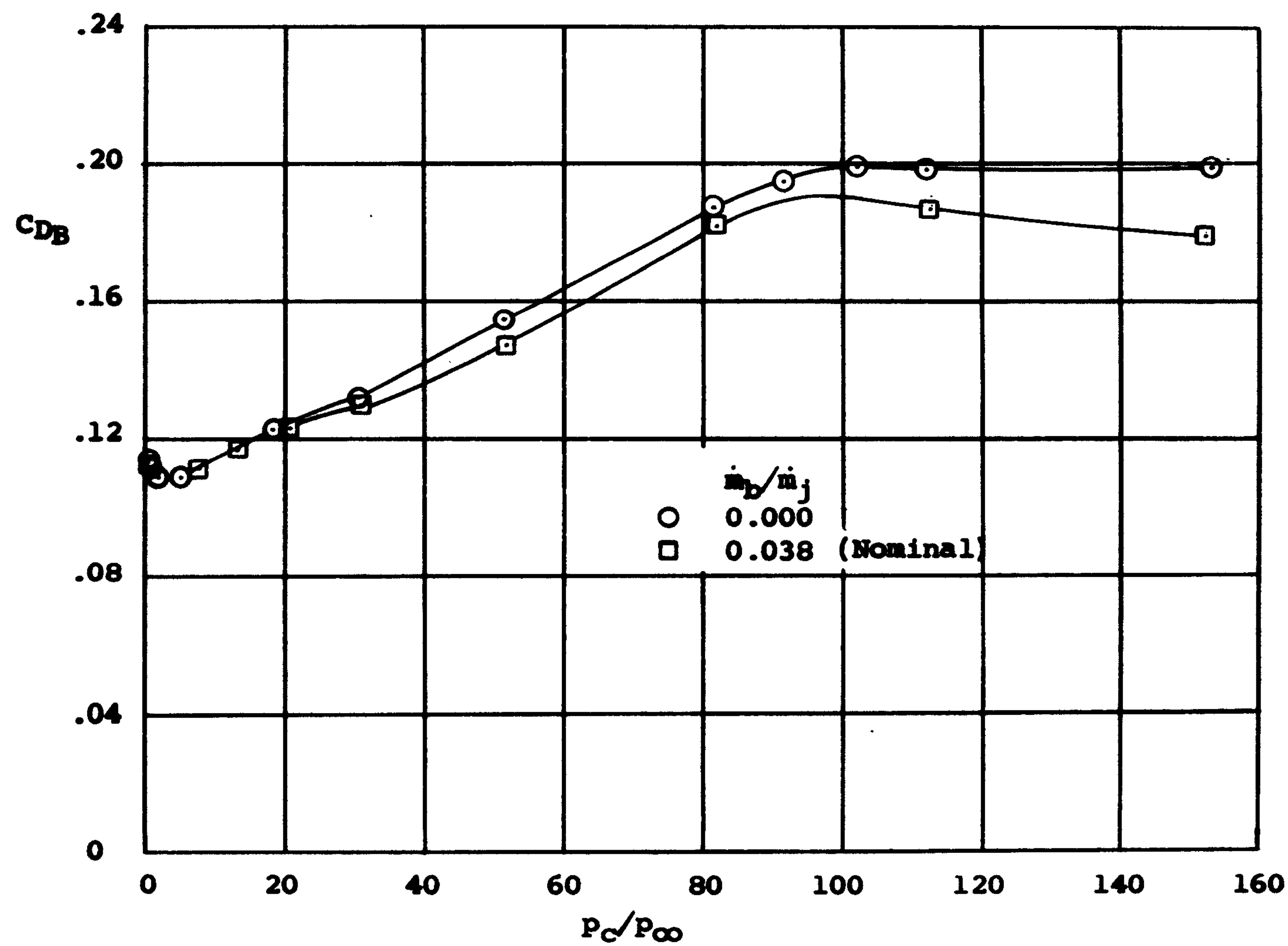

a. $d_n/D_B = 0.10$; $X_n/D_B = 0.0$

Figure 5. Effects of Base Bleed on Base Drag at M = 2.5

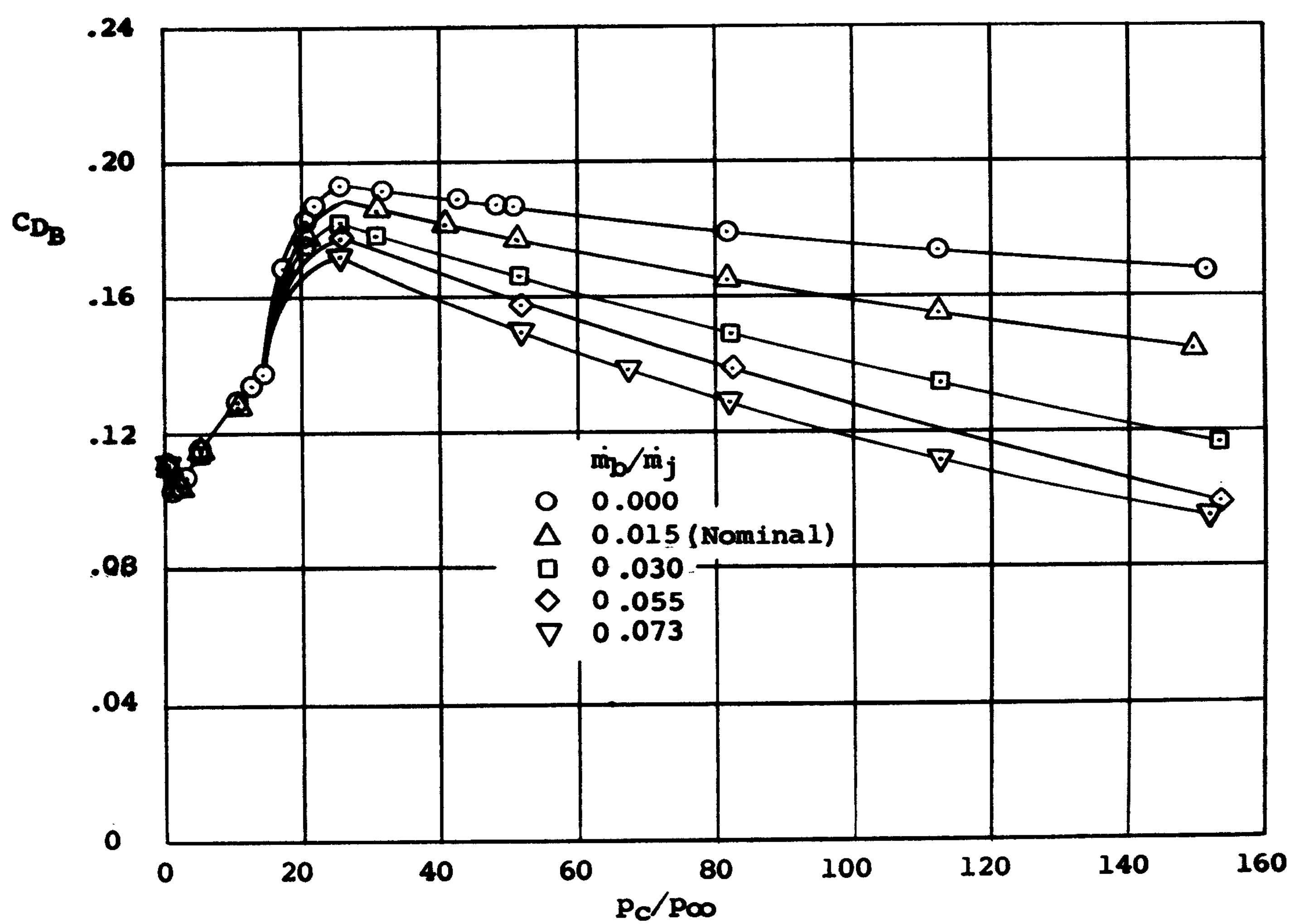

b. $d_n/D_B = 0.20$; $X_n/D_B = 0.0$

Figure 5. Continued

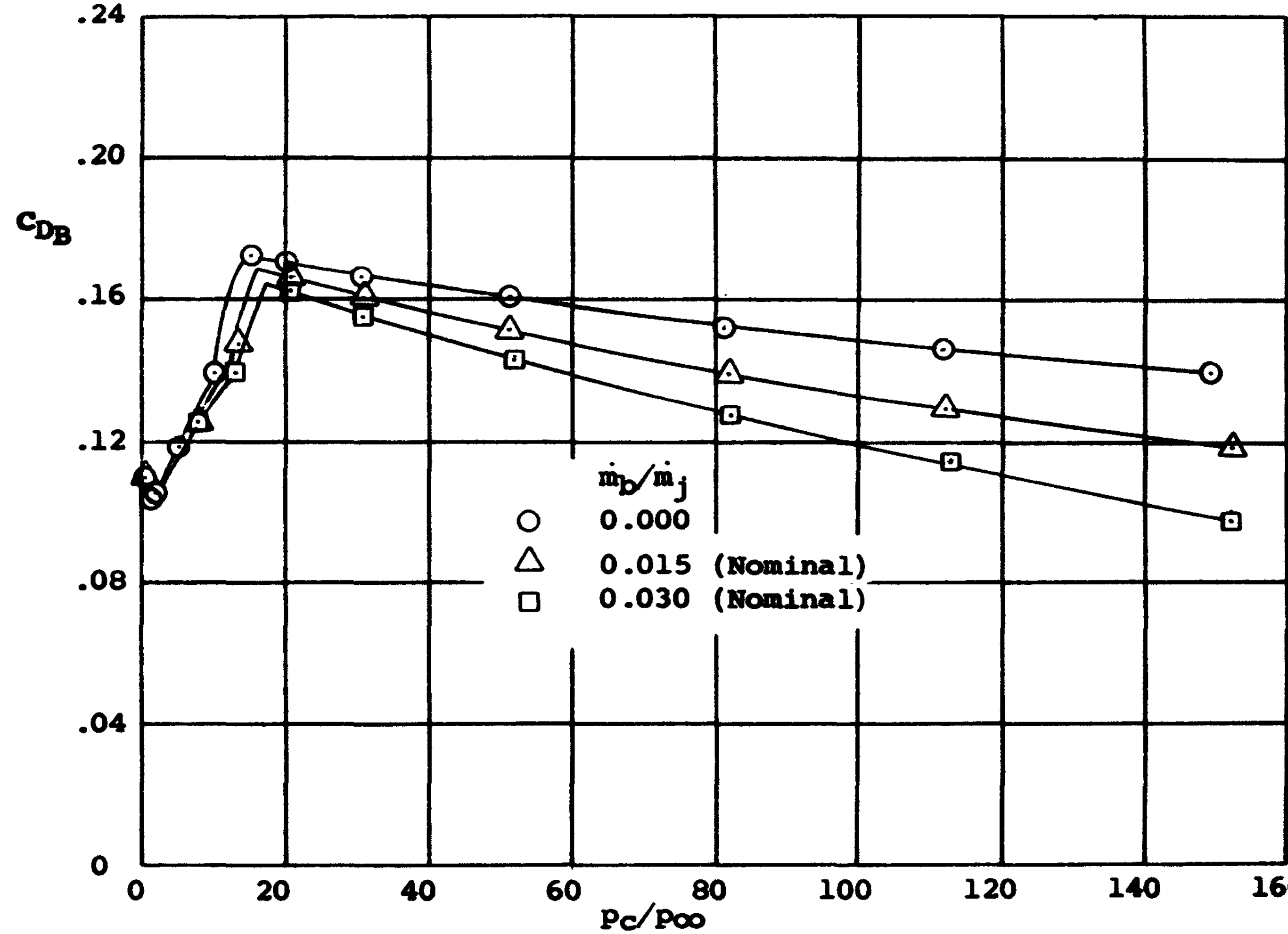

c. $d_n/D_B = 0.20;\ X_n/D_B = -0.40$

Figure 5. Continued

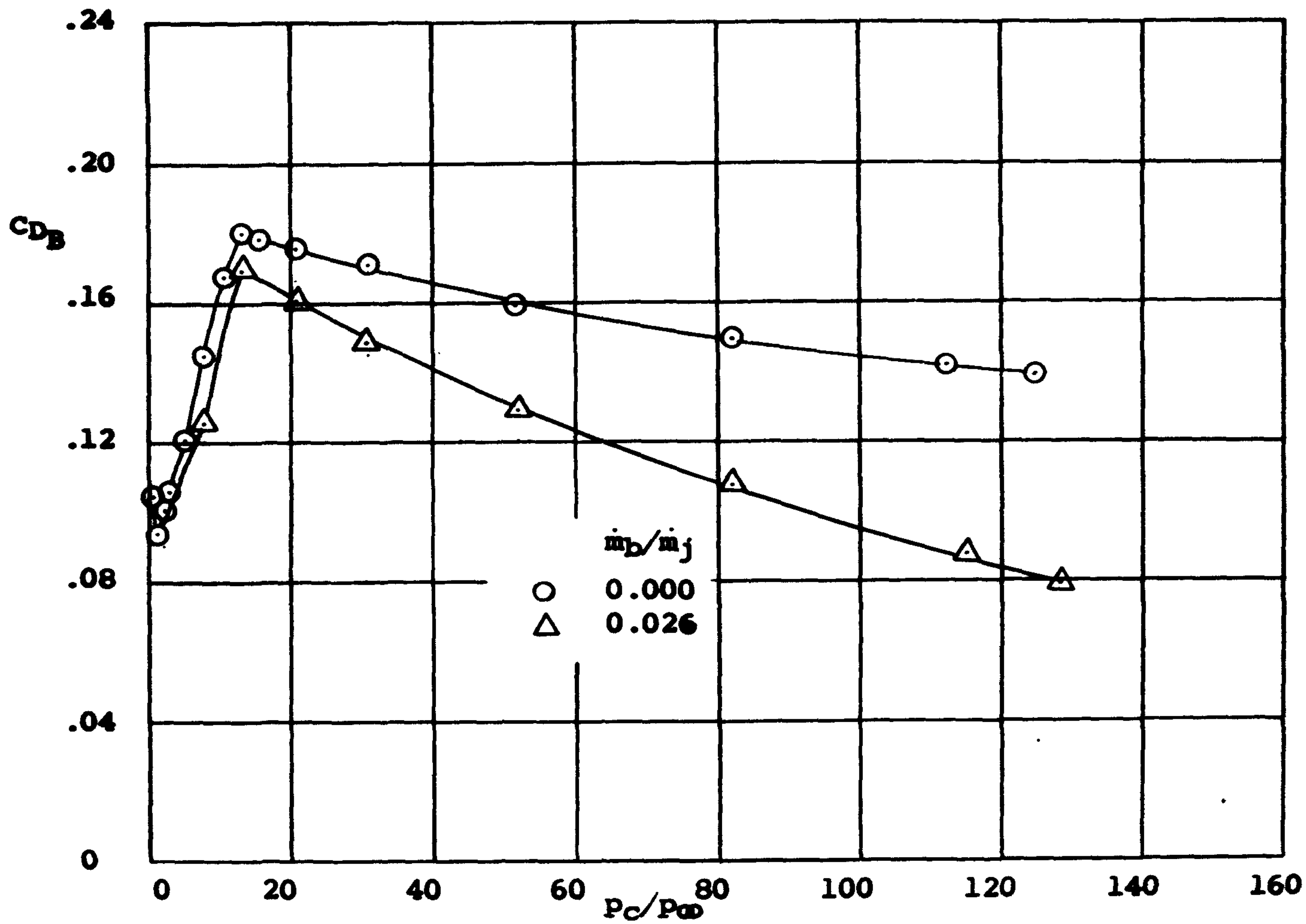

d. $d_n/D_B = 0.30$; $X_n/D_B = 0.00$

Figure 5. Continued

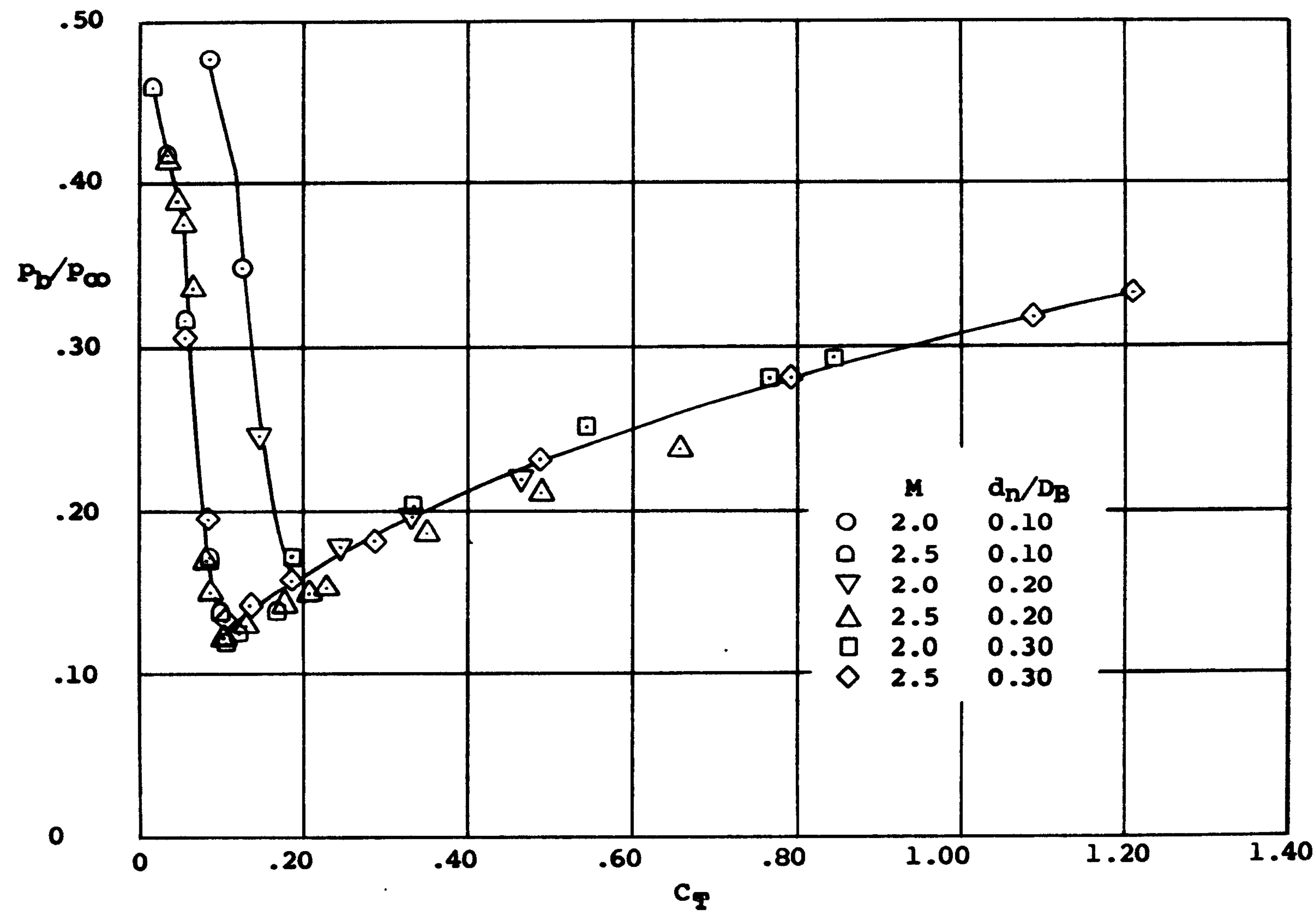

$X_n/D_B = 0.0$

Figure 6. Effects of Mach Number and Sustainer Nozzle Diameter Ratio on Base Pressure Ratio.

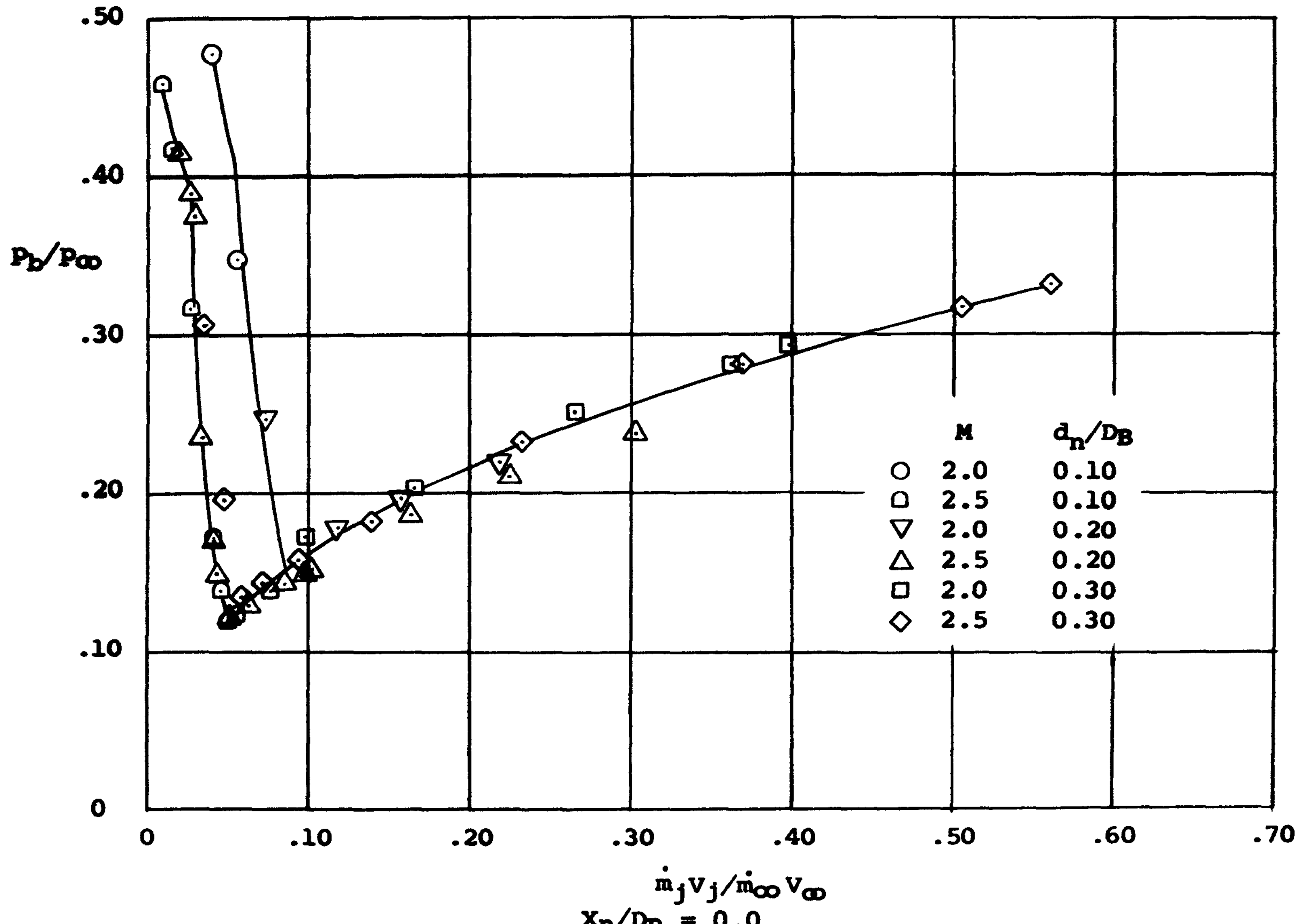

Figure 7. Effects of Mach Number and Sustainer Nozzle Diameter Ratio on Base Pressure Ratio.

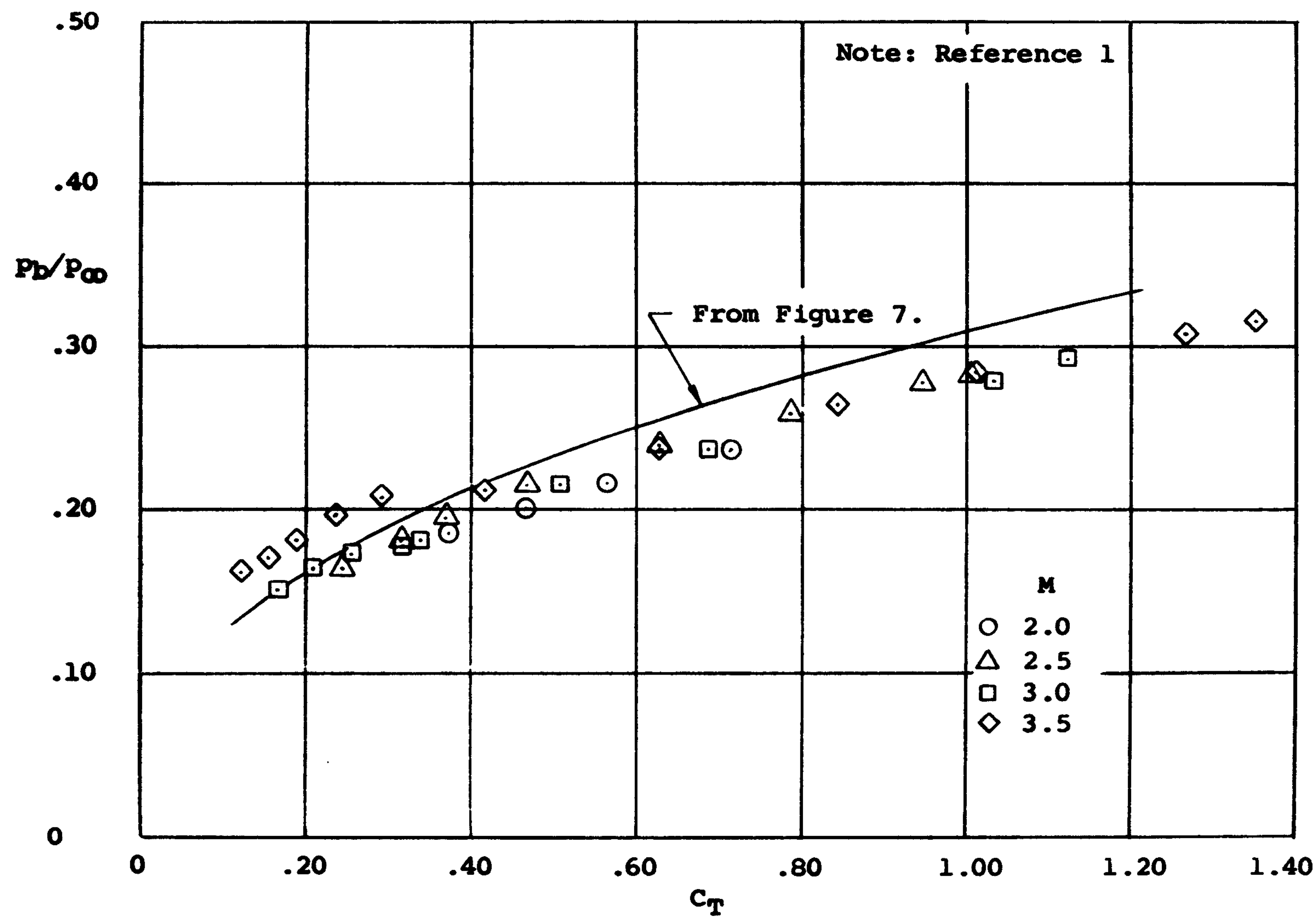

$X_n/D_B = 0.0; \quad d_n/D_B = 0.24$

Figure 8. Effects of Mach Number on Base Pressure Ratio

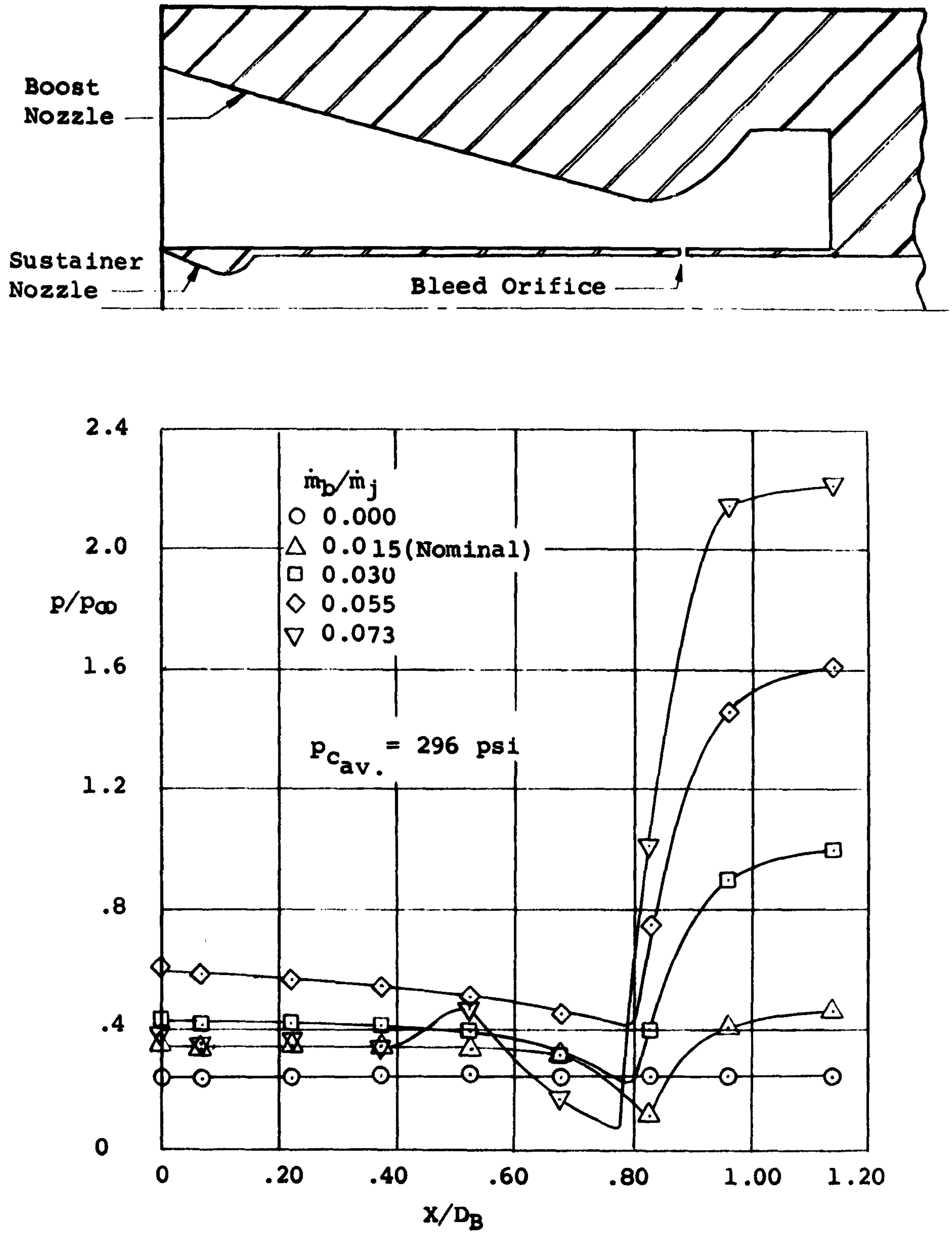

Figure 9. Effects of Bleed on Base Pressure Distribution.
$M = 2.5$; $d_n/D_B = .20$; $X_n/D_B = 0.00$

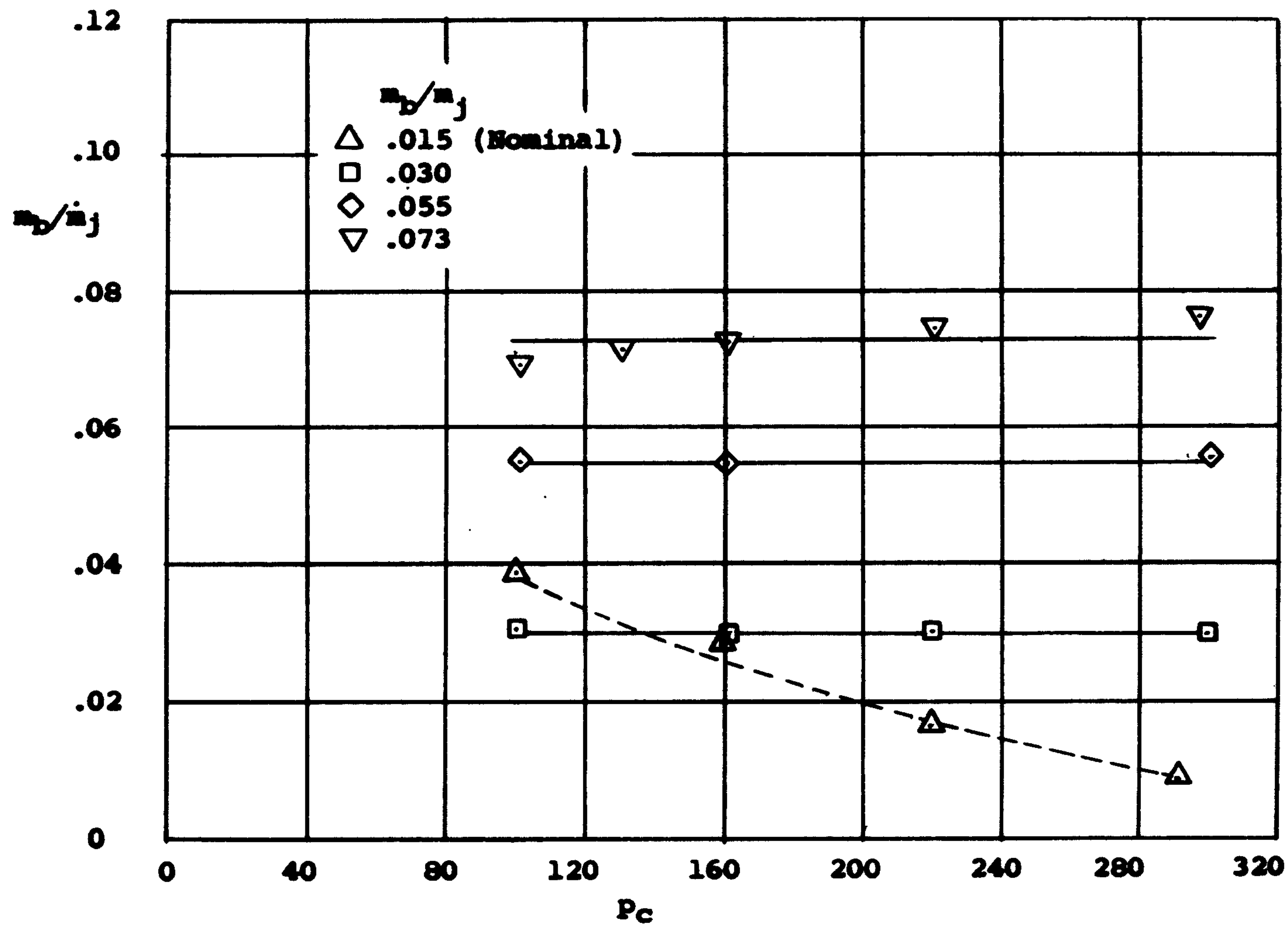

Figure 10. Variation in Bleed Mass Flow Ratio With Sustainer Jet Chamber Pressure $M = 2.5$; $d_n/D_B = .20$; $X_n/D_B = 0.00$

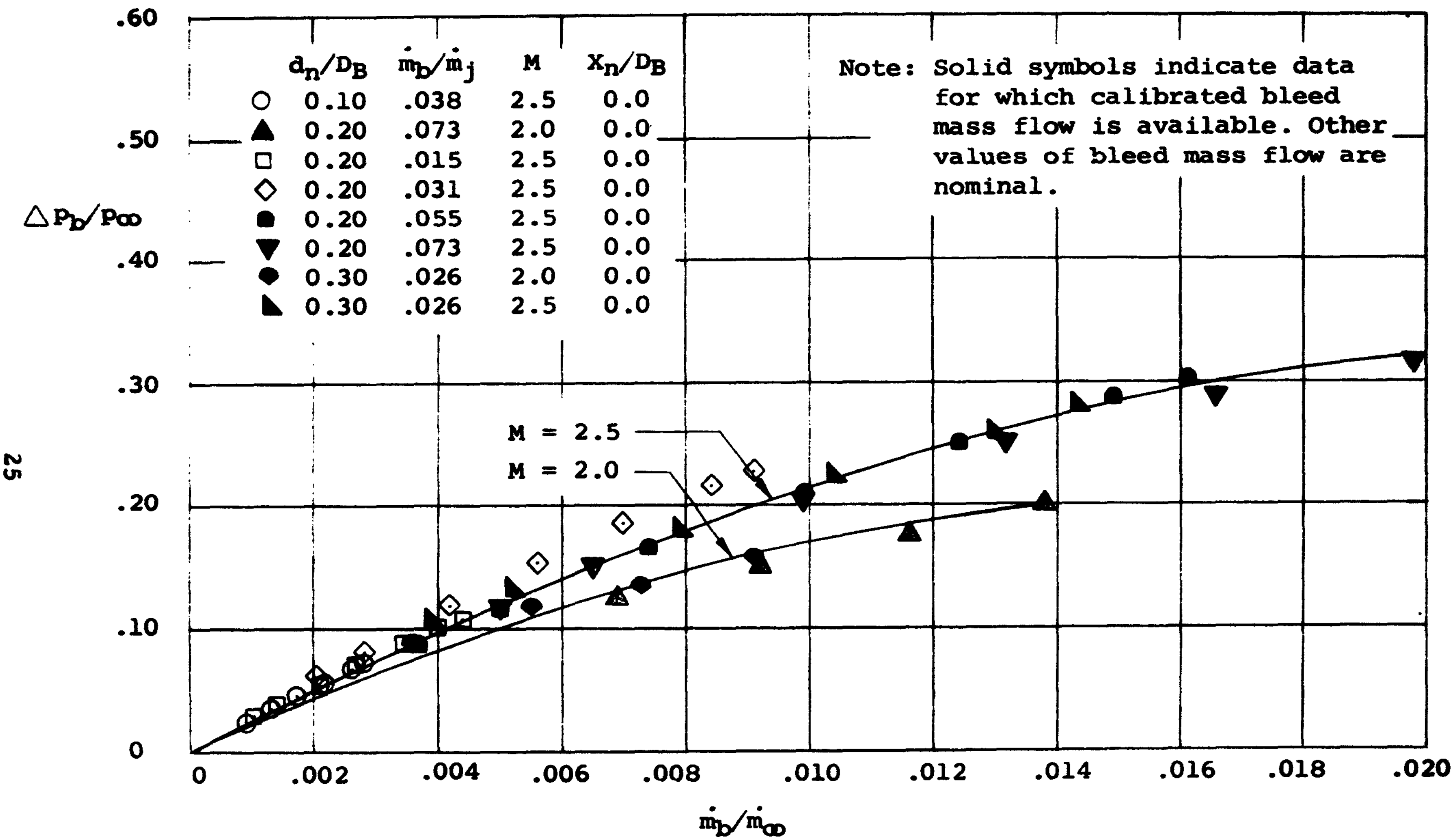

Figure 11. Increase in Base Pressure Ratio Due to Base Bleed.

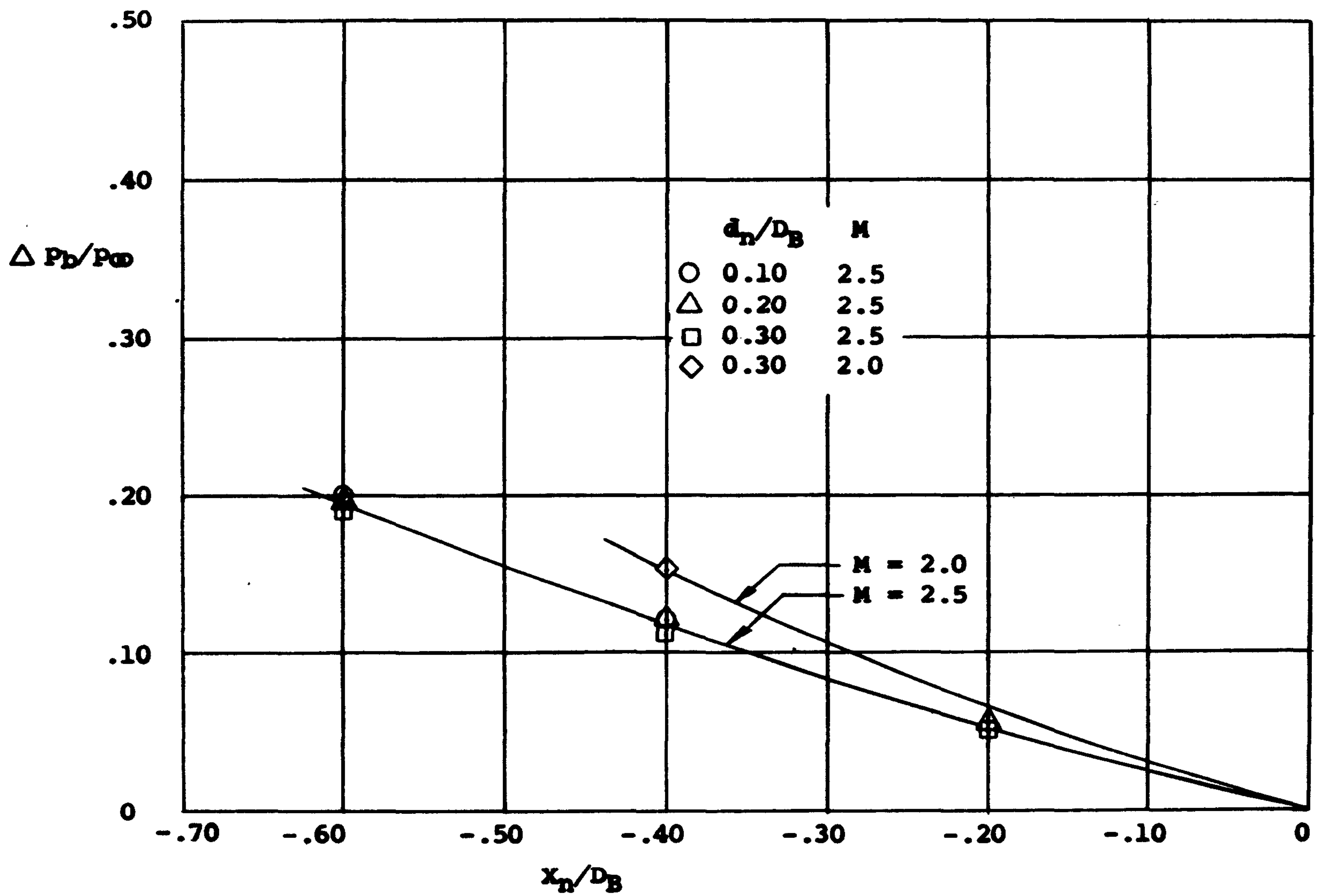

Figure 12. Increase in Base Pressure Ratio Due To Aft Nozzle Position.

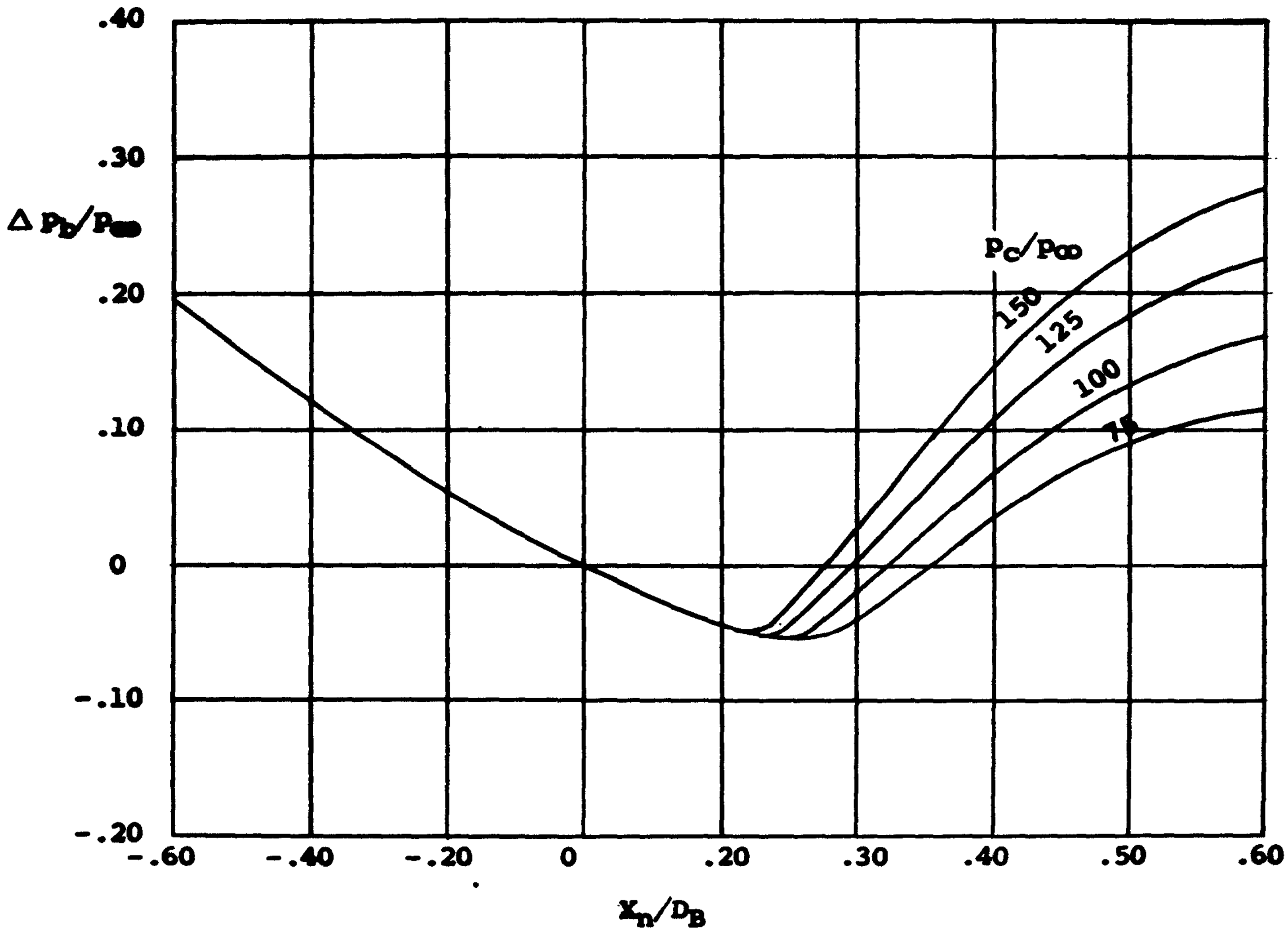

Figure 13. Incremental Change in Base Pressure Ratio Due to Sustainer Nozzle Position $M = 2.5$; $d_n/D_B = 0.20$

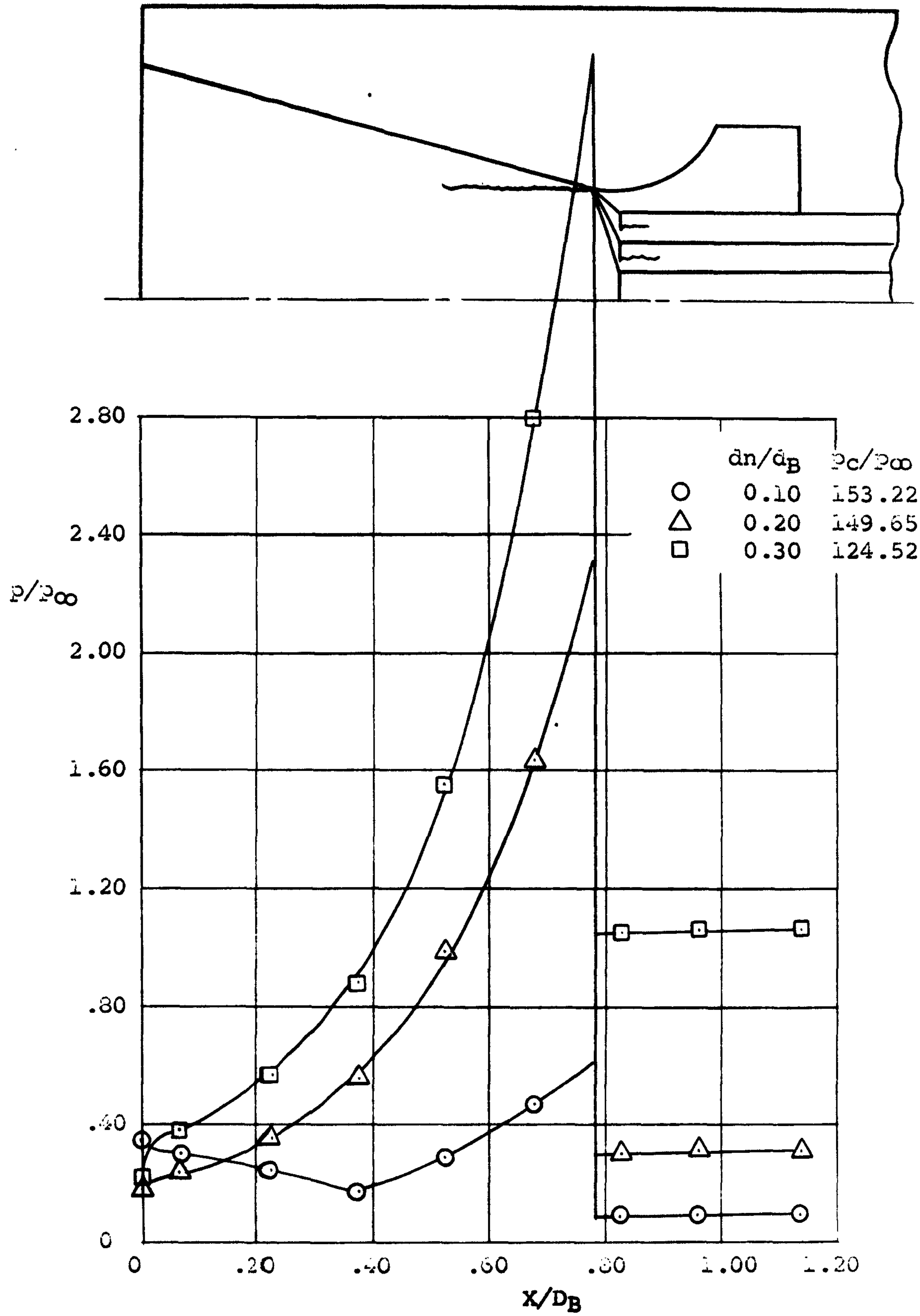

Figure 14. Effect of Sustainer Nozzle Diameter Ratio on Local Pressure Distribution. X_n/D_B = .8245; M = 2.5

REFERENCES

1. Brazzel, Charles E., "The Effects on Base Drag of Relative Longitudinal Arrangement of Concentric Boost and Sustainer Nozzles", AMICOM Report No. RF-TR-63-19, April 1963.

2. Blackwell, Kenneth L., "Some Effects of Nozzle Diameter and Position on Base Drag for Two Concentric Nozzles at Supersonic Mach Numbers", AMICOM Report No. RE-TM-63-25, 17 June 1963.

3. Reid, J., and Hastings, R.C., "The Effect of a Central Jet on the Base Pressure of a Cylindrical Afterbody in a Supersonic Stream", RAE Report No. AERO 2621, December 1959.

15 July 1963 Report No. RF-TR-63-23

APPROVED

James H. Henderson
JAMES H. HENDERSON
Chief, Analysis Section

Raymond A. Deep
RAYMOND A. DEEP
Chief, Aerodynamics Branch

William C. McCorkle Jr.
WILLIAM C. MCCORKLE, JR.
Director, Adv Sys Lab, FMSD

DISTRIBUTION

U.S. Army Missile Command Distribution List A for Technical Reports (11 March 1963)	1-103
Director of Defense Research and Engineering (OSD) Attn: Tech Library Room 3C128 The Pentagon Washington 25, D.C.	104
Commanding General U.S. Army Materiel Command Attn: AMCRD-RS-PE-Bal Res & Devel Directorate Washington 25, D.C.	105
Commanding General Picatinny Arsenal Attn: ORDBB-VC 3, Mr. A.A. Loeb Dover, New Jersey	106
Commanding Officer Frankford Arsenal Attn: 0270 - Library Philadelphia 37, Pennsylvania	107
Commanding Officer Ballistic Research Labs Attn: AMXBR-E Aberdeen, Maryland	108, 109
Chief, Bureau of Naval Weapons Attn: DIS-33 Department of the Navy Washington 25, D.C.	110-112
Naval Supersonic Laboratory Massachusetts Institute of Technology Attn: Mr. Frank Durgin 560 Memorial Drive Cambridge 39, Mass.	113
Chief of Naval Material Attn: Code M422 Department of the Navy Washington 25, D.C.	114
AFSWC (SWK, SWUND) Kirtland Air Force Base New Mexico	115
Commanding Officer and Director Attn: Aerodynamics Lab David W. Taylor Model Basin Washington 7, D.C.	116
Director, National Aeronautics and Space Administration Attn: Technical Library Ames Research Center Moffett Field, California	117-121
Director, National Aeronautics and Space Administration Attn: Technical Library Langley Research Center Langley Field, Virginia	122-126
Director, National Aeronautics and Space Administration Attn: Technical Library Lewis Research Center Cleveland, Ohio	127-131
Director, National Aeronautics and Space Administration Attn: W. Dahm E. Linsley J. Sims Marshall Space Flight Center Redstone Arsenal, Alabama	132-136
Director, National Bureau of Standards Attn: G.B. Schubauer 232 Dynamometer Bldg. Washington 25, D.C.	137
U.S. Atomic Energy Commission Tech Info Service Extension P.O. Box 62 Oak Ridge, Tennessee	138
National Science Foundation Attn: Dr. R. Seeger Washington 25, D.C.	139
Applied Physics Laboratory The Johns Hopkins University Attn: Mr. G. L. Seielstad 8621 Georgia Avenue Silver Spring, Maryland	140
Autonetics, A Division of North American Aviation, Inc. 9150 E. Imperial Highway Downey, California	141
AVCO Manufacturing Corp. Advance Devel Div Res Lab 2385 Revere Beach Parkway Everett 49, Mass.	142
Armour Research Foundation Illinois Institute of Technology Center Chicago, Illinois	143
Aerojet-General Corp Attn: Tech Info Office Sacramento Plants (Liquid & Solid Rocket Motors) P.O. Box 1947 Sacramento, California	144
American Bosch Arma Corp. Attn: Tech Library Roosevelt Field Garden City, New York	145
Bell Aircraft Corp. P.O. Box 1 Attn: Librarian Buffalo 5, New York	146
Bell Telephone Labs, Inc. Attn: Director of Military Systems Development Whippany, New Jersey	147
Bendix Corporation Attn: Reports Library Research Labs Division P.O. Box 5115 Detroit 35, Michigan	148
Boeing Company Attn: Library Unit Chief P.O. Box 3707 Seattle 24, Washington	149, 150
Bendix Mishawaka Division Attn: Tech Librarian Bendix Corporation 400 South Beiger Street Mishawaka, Indiana	151
Batelle Memorial Institute 505 King Avenue Columbus 1, Ohio	152
Bendix Corporation Bendix Systems Division Ann Arbor, Michigan	153
Beech Aircraft Corporation Wichita 1, Kansas	154
CONVAIR, A Division of General Dynamics Corp. P.O. Box 1950 San Diego 12, California	155
Cornell Aeronautical Lab, Inc. Attn: Librarian Buffalo, New York	156
CONVAIR, A Division of General Dynamics Corp. Attn: Engineering Librarian Fort Worth 1, Texas	157
Chance Vought Aircraft, Inc. P.O. Box 5807 Dallas, Texas	158, 159
CONVAIR, A Division of General Dynamics Corp. Attn: Division Library Pomona, California	160
Chrysler Corporation Attn: Tech Library Missile Operations P.O. Box 2628 Detroit 31, Michigan	161

Convair-Astronautics, Division of General Dynamics Corp.
Attn: Chief Librarian
San Diego 12, California — 162

Douglas Aircraft Company
Attn: Chief Engineer, Msls & Space Systems
3000 Ocean Park Blvd
Santa Monica, California — 163

Douglas Aircraft Company
Attn: R. L. Coleman, Aero Sec.
1820 Statesville Ave.
Charlotte, N.C. — 164

Documentation Inc.
Man-Machine Info Center
2521 Connecticut Ave., N.W.
Washington 8, D.C. — 165

Electronics Defense Lab
Sylvania Electric Products, Inc.
P.O. Box 205
Mountain View, California — 166

Fairchild Engine and Airplane Corp.
Fairchild Astronics Division
Wyandanch, Long Island
New York — 167

Fairchild Stratos Corp.
Aircraft-Missiles Division
Attn: Sarah M. Thomas Library
Hagerstown, Maryland — 168

Goodyear Aircraft Corp.
Akron 15, Ihio — 169

General Electric Company
Aircraft Products Dept
Lakeside Avenue
Burlington, Vermont — 170

Grumman Aircraft
Engineering Corp.
Attn: Director, Engineering Library, Plant 5
Bethpage, Long Island, New York — 171

General Electric Company
Attn: Tech Info Svcs
Tech Military Planning Operation
Box 535
Santa Barbara, California — 172

General Electric Company
Msl & Ord Systems Dept.
3198 Chestnut Street
Philadelphia, Pennsylvania — 173

General Electric Company
FPD Tech Info Center
Mail Stop F-22
Cincinnati 15, Ohio — 174

Hughes Aircraft Company
Attn: Documents Group Tech Library
Florence Ave. at Teale St.
Culver City, California — 175

Institute for Defense Analyses
Res & Eng Support Division
1825 Connecticut Ave., N.W.
Washington, D.C. — 176

Lockheed Aircraft Corp.
Attn: Tech Info Center
Msls I Space Division
P.O. Box 504
Sunnydale, California — 177

Librascope, Inc.
808 Western Avenue
Glendale I, California — 178

McDonnell Aircraft Corp.
P.O. Box 516
St. Louis 3, Missouri — 179

The Martin Company
Attn: Librarian
Orlando Division
Orlando, Florida — 180

The Martin Company
Attn: Research Library
Denver Division
P.O. Box 179
Denver 1, Colorado — 181

The Mitre Corp.
244 Wood Street
Lixington 73, Mass. — 182

Marquardt Aircraft Co.
16555 Saticoy Street
P.O. Box 2013 South Annex
Van Nuys, California — 183

Northrop Corporation
Attn: Tech Information
Norair Division
1001 East Broadway
Hawthorne, California — 184

North American Aviation, Inc.
Attn: Msl Devel Div.
12214 Lakewood Blvd.
Downey, California — 185

Nortronics, A Division of Northrop Aircraft, Inc.
Attn: Tech Info Center
222 North Prairie Ave.
Hawthorne, California — 186

Raytheon Company
Missiles Systems Division
Bristol, Tennessee — 187

Reeves Instrument Corp.
Ease Gate Blvd.
Garden City, Long Island, New York — 188

Raytheon Company
Attn: Librarian
Missile Systems Division
Bedford, Massachusetts — 189

Republic Aviation Corp.
Attn: Manager, Contracts and Liaison
Guided Missiles Division
Mineola, Long Island, New York — 190

Radio Corp. of America
Msl & Surface Radar Dept.
Moorestown, New Jersey — 191

Raytheon Company
Attn: Librarian
Andover Plant
Haverhill Street
Andover, Massachusetts — 192

Radioplane, A Division of Northrop Corp.
P.O. Box 511
Van Nuys, California — 193

Ryan Aeronautical Company
Attn: Chief Librarian
Lindbergh Field
San Diego 12, California — 194

Republic Aviation Corp.
Military Contract Dept.
Farmingdale, Long Island, New York — 195

Sylvania Electric Products, Inc.
Waltham Laboratory Library
Attn: Librarian
100 First Avenue
Waltham 54, Massachusetts — 196

Sperry Utah
Engineering Laboratory
322 North 21st Street, West
Salt Lake City 16, Utah — 197

System Development Corp.
Attn: Librarian
2500 Colorado Avenue
Santa Monica, California — 198

DISTRIBUTION - Continued

Sanders Associates, Inc.
Document Library
95 Canal Street
Nashua, New Hampshire
199

TEMCO Aircraft Corp.
Attn: Engineering Library
P.O. Box 6191
Dallas, Texas
200

United Aircraft Corp.
Missile and Space Division
400 Main Street
East Hartford 8, Conn.
201

United Aircraft Corp.
Research Department
East Hartford 8, Conn.
202

Vitro Laboratories
Div of Vitro Corp. of America
Attn: Librarian
14000 Georgia Avenue
Silver Springs, Maryland
203

Wright Aeronautical Division
Attn: Sales Dept (Fovt.)
Curtiss-Wright Corporation
Wood Ridge, New Jersey
204

Brown University
Attn: Dr. R. Probstein, Graduate Div.
of Applied Mathematics
Attn: Prof. William Prager, Chairman,
Physical Sciences Council
Providence 12, Rhode Island
205, 206

Catholic University of America
Attn: Prof. K.F. Herzfeld
Prof. M. Munk
Department of Physics
Washington 17, D.C.
207

Auburn University
Attn: Dept. of Aerospace Eng.
Auburn, Alabama
208

University of Alabama
Attn: Dept of Aerospace Eng
University, Alabama
209

Case Institute of Technology
Attn: Dr. G. Kuerti
Cleveland, Ohio
210

California Institute of Technology
Guggenheim Aeronautical Lab
Attn: Prof. H.W. Leipman
Pasadena 4, California
211

University of California at Berkeley
Attn: Prof. S.A. Schaaf
Berkeley, California
212

University of California at Los Angeles
Attn: Dr. L.M. Boelter
Dept. of Engineering
Los Angeles 24, California
213

University of Southern California
Engineering Center
Los Angeles 7, Caliornia
214

University of Chicago
Attn: Librarian
Labs for Applied Sciences
Museum of Science & Industry
Chicago 37, Illinois
215

Cornell University
Attn: Dr. W.R. Sears
Graduate School of Aeronautical Engineering
Ithaca, New York
216, 217

Harvard University
Attn: Prof. H.W. Emmons
Dr. A. Bryson
Prof. G.E. Carrier
Dept. of Applied Physics & Engineering Science
Cambridge 38, Massachusetts
218-220

University of Illinois
Attn: Prof. C.H. Fletcher
Dept. of Aeronautical Eng.
Attn: Dr. H.H. Korst
Eng. Experimental Station
Urbana, Illinois
221, 222

American Institute of Aeronautics & Astronautics
Attn: Library
2 East 64th Street
New York 21, New York
223

The Johns Hopkins University
Attn: Dr. L. Kosvasznay
Prof. F.H. Caluser, Jr.
Dept. of Aeronautical Eng.
Attn: Dr. S. Corrsin
Dept. of Mechanical Eng.
Baltimore 17, Maryland
224-226

Kansas State University
Attn: Prof. W. Tripp
Dept. of Mechanical Eng.
Manhattan, Kansas
227

Lehigh University
Attn: Dr. R. Emrich
Physics Dept.
Bethlehem, Pennsylvania
228

University of Maryland
Attn: Director, Institute of Fluid
Dynamics & Applied Mathematics
Attn: S.F. Shen, Dept. of Aeronautical Eng.
College Park, Maryland
229, 230

University of Michigan
Institute of Science & Technology
Attn: Tech Documents Service
Ann Arbor, Michigan
231

Massachusetts Institute of Technology
Attn: Prof. J.R. Markham
Dept. of Aeronautical Eng.
Cambridge 39, Mass.
232

University of Michigan
Attn: Dr. Arnold Kuethe
Dept. of Aeronautical Eng.
East Engineering Bldg.
Ann Arbor, Michigan
233

University of Minnesota
Attn: Dept. of Aeronautical Eng.
Dept. of Mechanical Eng., Div. of Thermodynamics
Minneapolis 14, Minn.
234, 235

Midwest Research Institute
Attn: M. Goland, Director for Engineering Sciences
4049 Pennsylvania
Kansas City 11, Missouri
236

New York University
Attn: Dr. R.W. Courant, Institute of
Mathematics & Mechanics
Attn: Dr. J.F. Ludloff, Dept. of Aeronautics
45 Fourth Street
New York 53, N.Y.
237, 238

North Carolina State College
Attn: Prof. R.M. Pinkerton
Dept. of Engineering
Raleigh, North Carolina
239

Ohio State University
Attn: Prof. G.L. von Eschen
Aeronautical Engr. Dept.
Columbus, Ohio
240

Pennsylvania State College
Attn: Prof. M. Lessen
Dept. of Aeronautical Engr.
State College, Pennsylvania
241

Polytechnic Institute of Brooklyn
Attn: Dr. A. Ferri
Aerodynamic Laboratory
527 Atlantic Avenue
Freeport, New York
242

Princeton University Attn: Prof. S. Bogdonnoff Prof. W. Hayes Forrestal Research Center Princeton, New Jersey	243, 244
Purdue University Lafayette, Indiana	245
Princeton University Forrestal Research Center Library Project SQUID Princeton, New Jersey	246
The Rice Institute Attn: Prof. A.J. Chapman Dept. of Mechanical Eng. Houston, Texas	247
Rensselaer Polytechnic Institute Attn: Dr. R.P. Harrington Aeronautics Department Troy, New York	248
Rutgers University Attn: Prof. R.H. Page Dept. of Mechanical Engr. New Brunswick, N.J.	249
Stanford Research Institute Attn: Acquisitions Documents Center Menlo Park, California	250
University of Virginia Ordnance Research Laboratory P.O. Box 3366 University Station Charlottesville, Virginia	251
University of Texas Defense Research Laboratory Attn: Mr. J.B. Oliphint P.O. Box 8029 University Station Austin 12, Texas	252, 253
University of Washington Attn: Prof. R.E. Street Department of Aeronautical Engr. Attn: Prof. M.E. Childs Dept. of Mechanical Engr. Seattle 5, Washington	254, 255
Prof. J.W. Beams University of Virginia Department of Physics Charlottesville, Virginia	256
Dr. E.R. Benton University of Manchester, England	257
Dr. R. Bolz Case Institute of Technology Cleveland, Ohio	258
Mr. Gerald Hieser Systems Engineering Dept. General Electric Company 21 South 12th Street Room 514 Philadelphia, Pennsylvania	259
Prof. J.O. Hirschfelder University of Wisconsin Department of Chemistry Madison, Wisconsin	260
Prof. C.B. Millikan Director, Guggenheim Aeronautical Laboratory California Institute of Technology Pasadena 4, California	261
Dr. Henry F. Hrubecky Dept. of Mechanical Engineering Tulane University New Orleans 18, La.	262
Commanding General U. S. Army Materiel Command Attn: AMCRD-BE, Mr. Stetson Attn: AMCRD-BE-MI, Mr. Michaels Research & Development Directorate Washington 25, D. C.	263 264
AMSMI-R, Mr. McDaniel	265
-RF, Mr. Hussey	266
-RFS, Record Copies	267-269
-RFSK, Mr. Deep	270
-RFSK, Mr. Henderson	271
-RFSK, Mr. Brazzel	272-292
-RFSK, Mr. Johnson	293
-RFSK, Mr. Street	294
-RFSK, Mr. Greene	295
-RFSK, Mr. Becht	296
-RFSK, File Copy	297
-RBL	298-302
-RG	303
-RK	304
-RE	305
-RFE, Mr. Garner	306
-RT	307
-RH	308
-RL	309
-RR	310
-RS	311
-RAP	312